Int. J. Electrochem. Sci., 10 **(2015)** 7111 - 7137

International Journal of
ELECTROCHEMICAL
SCIENCE
www.electrochemsci.org

Review

Enhancement of Different Fabricated Electrode Materials for Microbial Fuel cell Applications: An Overview

Rasu Ramachandran[1], *Shen-Ming Chen*[2,*], *George peter Gnana kumar*[3]

[1]Department of Chemistry, The Madura College, Vidya Nagar, Madurai – 625 011, Tamil Nadu, India.
[2]Electroanalysis and Bioelectrochemistry Lab, Department of Chemical Engineering and Biotechnology, National Taipei University of Technology, No.1, Section 3, Chung-Hsiao East Road, Taipei 106.Taiwan (ROC).
[3]Department of Physical Chemistry, School of Chemistry, Madurai Kamaraj University, Madurai-625 021,Tamil Nadu, India.
[*]E-mail: smchen78@ms15.hinet.net

Received: 24 May 2015 / *Accepted:* 23 June 2015 / *Published:* 28 July 2015

This paper overviews around 125 research article's fundamentals, methods of preparation of electrode catalysts, characterization techniques, optimized parameters, electrode stability and electrode catalytic activities for the microbial fuel cell applications. Previously, platinum-based electrode catalysts have been used as both anode and cathode electrode catalysts in MFC analysis, but the available source is limited and high cost. Recently, nanocomposite (Metal, carbon, metal oxides and conducting polymer) based electrode catalysts were assembled with MFC for the usage of wastewater treatment and green energy power production. These kinds of composites were high electrode-surface area, environment friendly, commercially available, alternative Pt electrode and inexpensive. Therefore, this review is fully focused on the electrocatalytic activity of most conversion energy efficiency in MFC power production. In this article overviews, the current-state-of-art is highlighted, most probably develop a new strategy of scientific analysis and the improvement of power performance for enhancing the MFC catalytic activities.

Keywords: Electrode materials, Electroanalytical methods, Electrochemistry, Microbial Fuel cell, Bacteria.

1. INTRODUCTION

Microbial fuel cells (MFCs) are mainly obtained from the organisms of electrochemically active bacteria and biodegradable organic substrates and their metabolism to generate the sustainable and green energy for the conversion of chemical energy into electrical energy. The major conversion

of MFC through the bio electrochemical reaction can be used as a most promising green energy storage device to fulfil the energy crises. There has been extensive growth of MFC and green energy technology in the last decade, primarily because of the availability of viable methods for the synthesis of carbon, metal oxides, conducting polymer and nanocomposite based electrode materials as well as new tools for the characterization. Zhang *et al* [1] used an inexpensive carnation-like MnO_2 modified activated carbon (MnO_2 AC) air cathode prepared using the electro deposition method, which could obtain the reported maximum power density value of 1554 mW m^{-2}. In an MFC, the control geometrical properties of MWCNTs were direct interactions between physical and electrochemical microprobes and electrode surface. The anode materials based MWCNT composite showed highest power production (3360 mW m^{-2}) performance ie the power density value was 7.4-fold higher than the bare carbon cloth electrode [2]. A number of excellent reviews have been discussed (overviewed) for the effect of various optimized parameters (pH, temperature and loading rate) conditions to increase their expected power production rate. In addition to the continuing challenges and effective treatment of different methods for producing different structural oriented electrode materials, which were applied in MFCs applications [3,4,5,6]. The new development of a vertical substrate flow constructed granular activated carbon (GAC) was modified with stainless steel mesh (SSM) electrode. The bio-cathode (GAC-SSM) exhibited the highest power density value of 55.05 mW m^{-2} [7]. MFC consists of carbon felt-supported nano molybdenum carbide (Mo_2C) based carbon nanotube (CNT) (Mo_2C/CNT) nanotube composite has been synthesized by using microwave-assisted method. The Pt-free anode electrode (Mo_2C/CNT) catalyst exhibits superior performance of the developed conversion of organic substrate into electricity through *E-Coli* bacteria [8]. The most commonly used graphene based (Crumpled and flat sheet) electrode catalysts have been widely used in MFC applications. In this case, the crumpled graphene electrode catalyst was obtained large surface area, high electrical conductivity and excellent catalytic activity towards oxygen reduction reaction. The crumpled-graphene based anode electrode was exhibited better electrochemical performance (3.6 W m^{-3}) and greatly reduced the impedance than that of activated carbon (1.7 W m^{-3}) [9]. The electro active bifunctional quaternary ammonium compound has been explored extensively hinder bio-film growth and enhanced their power performance [10]. Zhao *et al* [11] have used as an inexpensive and easy approach for the development of iron (II) phthalocyanine (FePc) and cobalt tetramethoxyphenylporphyrin (CoTMPP) based oxygen reduction catalyst act as a cathode material in an MFC application. However, MFC of an algae (*Chlorella vulgaris*)-assisted cathode materials could also be enhanced the appreciable power generation (21 mW m^{-2}) of the sediment microbial fuel cell (SMFC) and it was further increased (38 mW m^{-2}) when CNT added on the cathode electrode surface [12]. Another important MFC application involves the use of surface modified carbon cloth anode have been optimized by four different methods, such as soaking in ammonia (CC-A), phosphate buffer (CC-P), nitric acid (CC-N) and nitric acid followed by soaking of aqueous ammonia (CC-NA). Among these electrode catalysts, MFC with anode modified CC-NA reported maximum power density value (3.20 ± 0.05 W m^{-2}) than the CC-C (2.01 ± W m^{-2}) value. In this result has been demonstrated to be primarily attributed to the enhancement of electron transfer was occurring from quinoid group on the CC-NA surface [13]. Ammonia treated (700º C) commercially available activated carbon (AC) powders have produced maximum power density (2450 ± 40 mW m^{-2}) than that of untreated AC (2100 ± mW m^{-2}) cathode

[14]. An electrochemical active nano covalent functionalized graphene modified iron tetrasulfophthalocyanine (FeTsPc-graphene) nanocomposite has been prepared by non-covalent method. Nevertheless, FeTsPc-graphene composite can be used as an alternative Pt-free catalyst in MFC studies [15]. The growth of modified electrode catalysts has been much effectively electrochemically developed in both theoretical and experimental methods. Especially, these kinds of electrode catalysts were extensively applied in various fields such as pesticide sensor [16], sensors [17], bio-sensors [18], supercapacitor [19] and solar cells [20].

In this perspective review, we have specifically focused on various synthesis methods for producing different types of electrode catalysts, optimized parameters (pH and temperature) and assorted electrochemical techniques have been used for the estimation of high power production (Green energy) through MFCs.

2. ELECTRODE CATALYSTS

2.1. Carbon

There have been some studies on the application of microbial fuel cell (MFC) in various electrode materials. Deng [21] have examined activated carbon fiber felt (ACFF) in various configuration forms like tubular and granular structures. The tubular shaped ACFF produced maximum power density value (784 mW m^{-2}) than granular ACFF (667 mW m^{-2}). A systematic study of carbon-based anode catalyst has been used for MFC with *Shewanella oneidensis MR-1*. The half-cell polarization curve analysis of the activated carbon material showed significantly better anode performance and high current density value than bucky paper, graphite felt and carbon paper [22]. The multi-scale forming nickel (Ni) supported web of activated carbon fiber (ACFs) modified with carbon micro-nanofibers (CNF) has been prepared by chemical vapor deposition method using Ni nanoparticle as the catalyst and benzene as the carbon source for the grow of CNFs and ACF substrate. The exhibited (open circuit potential) OCP and the current density of Ni-ACF/CNF base MFC were estimated to be 710 ± 5 mV and 1145 ± 20 mW m^{-2} [23]. Wei *et al* [24] have examined the two kinds of inexpensive semi coke and activated carbon bed bio-cathode materials were used for oxygen reduction reaction in MFC. The MFC of semi coke and activated carbon reported the high power density value of 20.1 W m^{-3} and 24.3 W m^{-3} respectively. A novel MFC study pertaining to the various deposition of Pt on carbon cloth materials such as electrodeposition, e-gun and sputter coating methods. By using XPS analysis, the amount of Pt(0) and zero-valent Pt deposited on the carbon cloth by electrodeposition was larger than that by *e*-gun and sputter coating methods. The same results were observed from the impedance analysis. Therefore power performance of MFC showed, electrodeposited method revealed higher power density value than others [25]. Kara *et al* [26] reported that carbon fiber brush (CB) and activated carbon nanofiber (ACNF) electrodes have been used for benthic microbial fuel cell (BMFC). Similarly, granular activated carbon (GAC) which can be used as a model anode in underwater BMFC, high mechanical strength and long-term durability in benthic applications. The carbon black (CB) electrode could be modified with iron phthalocyanine (FePc)

(CB/FePc) composite catalyst exhibited lowering of potential value (606 mV) than the previously reported nanotube based phthalocyanine composite (620 mV). The CB/FePc composite can be modified with Enterobacter cloacae and it provided greater power density values than unmodified one [27].

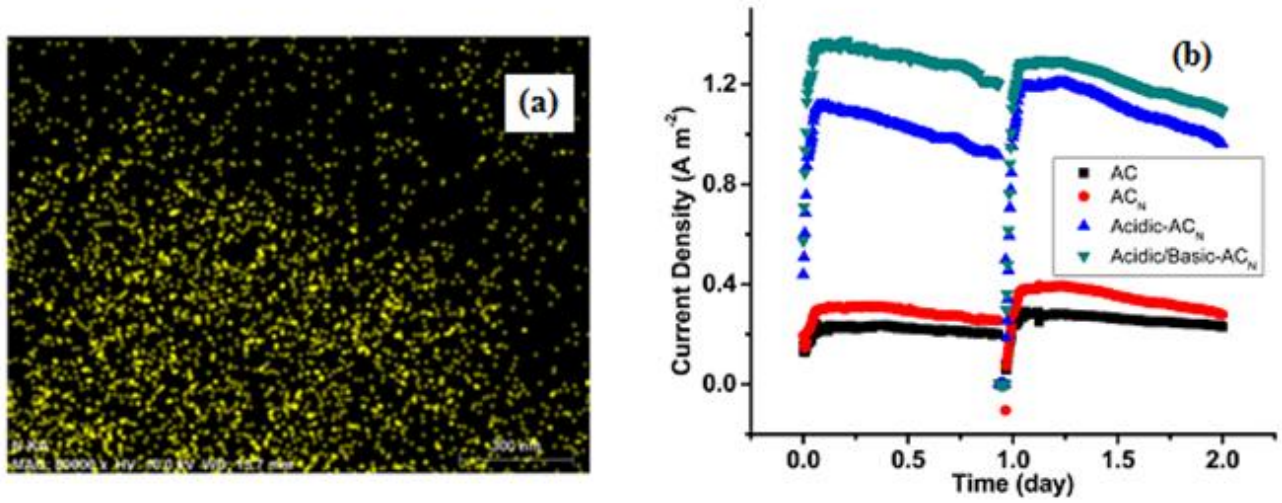

Figure 1. (a) Bright-field image carbon and nitrogen (b) Profile of the current generation in the MFCs with different AC catalysts. ("Reprinted with permission from (*ACS Appl. Mater. Interfaces* 6 (2014) 7464-7470). Copyright (2014) American Chemical Society").

Zhang *et al* [28] have used nitrogen-doped activated carbon catalyst for oxygen reduction in MFCs. Fig.1. (a) Shows that SEM image of yellow dots was attributed to the carbon and nitrogen. Comparison of different electrode catalysts, especially Pt/C cathode reported maximum power density (0.45 ± 0.40 W m^{-2}) value (Fig.1.b).

2.2. Carbon nanotubes

Sun and his co-workers [29] pioneered the use of MFC in electrochemical applications. The multi-walled carbon nanotube modified with polyelectrolyte polyethyleneimine (PEI) composite has been synthesized by a layer-by-layer self-assembled method. MFCs are attractive, the EIS analysis measured the existence of PEI/MWCNT composite decreased the RCT value in the range from1163 to 258 Ω and it can be produced the reported higher power density value with 20% enhancement. The power density value of the Pt supported carbon nanotube based nanofluid electrode was found to be much higher (2470 mW m^{-2}) value than the unmodified graphite electrode by dispersing nanocrystalline platinum anchored carbon nanotube. By this electrode catalyst performance of *E-Coli* based MFC has been demonstrated [30]. The composite of polypyrrole (PPy) and CNT (PPy/CNT) synthesized by *in situ* chemical polymerization method of pyrrole and CNT, the *E-Coli* used as a biocatalyst. The prepared composite electrode materials showed tubular morphologies and the mediatorless MFC of PPy/CNTs exhibited maximum power density value of 228 mW m^{-2} [31]. He *et*

al [32] have recently reported that carbon nanotube catalyst can serve as an excellent up flow fixed bed microbial fuel cell (FBMFC) for continuous treatment of waste water and electricity generation application. Notably, CNT exhibit a maximum power density value of 590 mW m^{-3} and it was achieved with a maximal chemical oxygen demand (COD). The organic loading rate (OLR) of 10.27 g COD l^{-1} d^{-1} caused by the overloading of MFC. This type of overloading MFC to improve the performance of FBMFC for energy production.

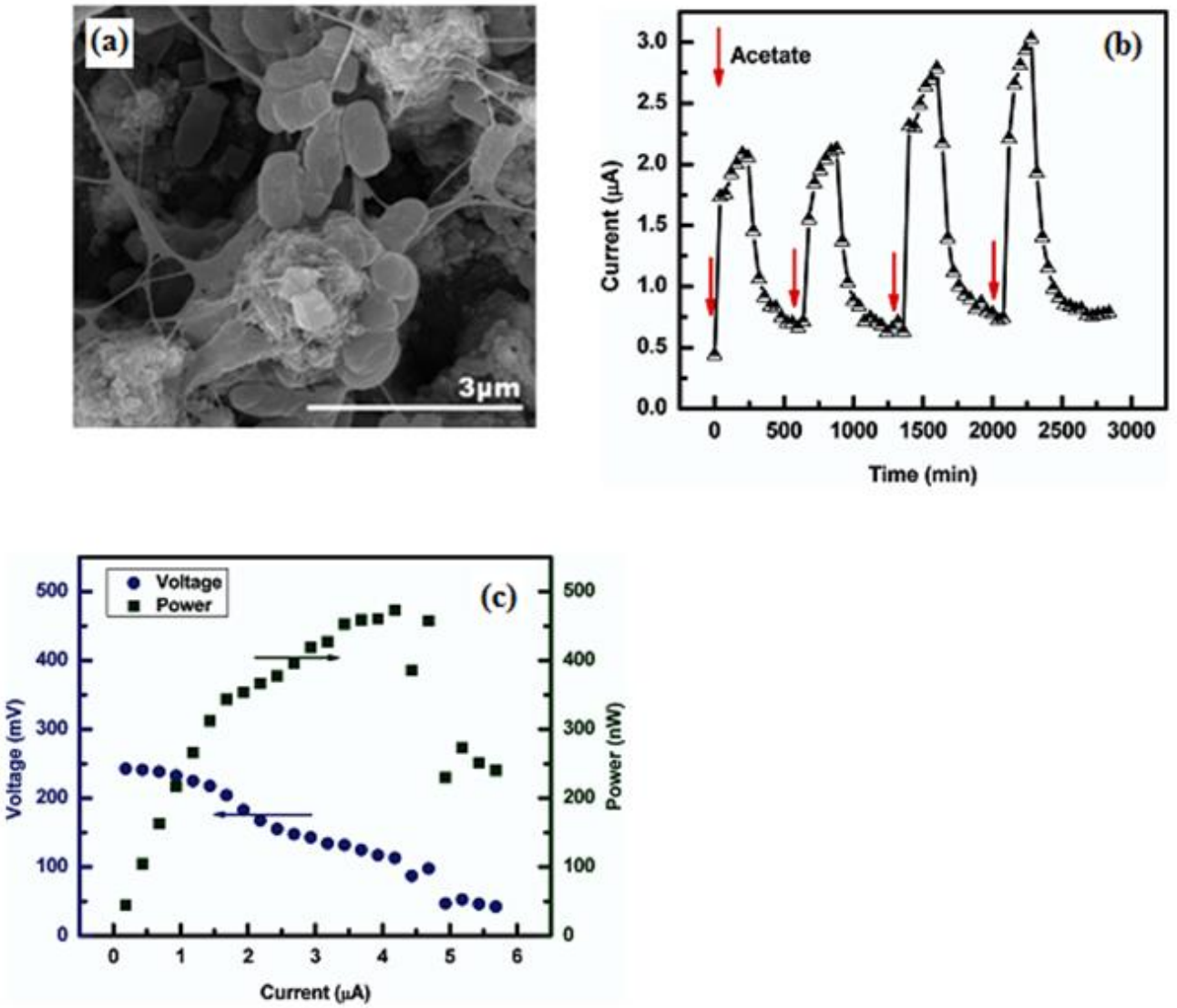

Figure 2. (a) Scanning electron microscopic (SEM) zoomed excellent compatibility with MWCNT (b) Current generation *vs* time plot showing a steady rise in current and short start-up time, Data shown 15 h after initial acetate introduction when stable cycles began. (c) Polarization plot of the 1.25 µL MFC. ("Reprinted with permission from (*Nano Lett*. 12 (2012) 791-795). Copyright (2012) American Chemical Society").

A three-dimensional nanostructure of carbon nanotube-gold-titania (CNT/Au/TiO_2) nanocomposite used as an anode material. This composite could utilize a new effective microbial fuel

cell (MFC) analysis and the relevant composite exhibit high conductivity, high specific area and easily adsorption of microorganism. The MFC equipped with CNT/Au/TiO_2 nanocomposite modified anode, the estimated power density value of 2.4 mW m^{-2}, which was three times higher than that of the bare carbon paper electrode [33]. Dip-coating is a viable method to form reduced graphene oxide and carbon nanotube (*r*GO-CNT) sponges of optimized thickness layer one. The 1.5 nm thickness of thinnest catalyst exhibited better performance, maximum power density (335 A m^{-3}) and remarkable cycle stability of 20 days at 37º C [34]. The highest electrochemical enhancement activity was mainly due to their inherent properties of amino functionalized multi-walled carbon nanotube and iron phthalocyanine (*a*-MWCNT/FePc) composite for oxygen reduction reaction (ORR) in air-cathode MFC. Electrochemical techniques (Cyclic voltammetry and linear sweep voltammetry) have been used to optimize the electrochemical properties. The main achieved power density value of 601 mW m^{-2} from MFC with *a*-MWCNT/FePc composite [35]. Development of vertically aligned MWCNT with nickel silicide (NiSi) could facilitate the enhanced power production of MFC. The high magnification of SEM image showed excellent compatibility with MWCNT (Fig.2.a).

The current generation plot was increased, when added to acetate solution and this cycle was stable up to 15 h (Fig.2.b). Energy loss (1.25 μL) also can be calculated from the polarization slope in Fig.2.c [36].

2.3. Graphene oxides

The wrinkled and crumpled morphological structure of electrochemically reduced graphene oxide (ERNGO) and polyaniline coating on carbon cloth (CC) surface (PANI/ERNGO/CC). The nanocomplexes composite have much better power density value (1390 mW m^{-2}) than the other MFC with CC anode [37]. Zhang *et al* [38] used three different anodic electrode catalysis of MFC based on Escherichia coli (ATCC25922), such as plain stainless steel mesh (SSM), polytetrafluoroethylene (PTFE) modified SSM and graphene modified SSM (GSM) etc. The smooth surface of graphene modified (GMS) anode catalyst to improve the power density (2668 mW m^{-2}) of an *E-Coli* catalyst MFC and the estimated BET surface area value of 264 m^2 g^{-1}. Studies on the applications of electrochemically prepared carbon cloth based graphene composite catalyst in MFCs. The graphene modified catalyst has been focused on the improvement of power density and energy conversion efficiency value by 2.7 and 3 times respectively. This result has been demonstrated that graphene electrode suggested a low cost fabrication method and it exhibit high power MFC applications [39]. On the other hand, a new composite of reduced graphene oxide/tin oxide (RGO/SnO_2) anode have also been explored to improve their power output of MFC. The fabricated RGO/SnO_2 anode plays an important role in influencing the catalytic activity of the bacterial bio film formation [40]. The globular structured materials of polypyrrole (PPy), graphene oxide (GO) and graphite felt (GF) has been used to modify the MFC electrode to maximize the surface area, electronic conductivity, biocompatibility and high stability as compared to the unmodified (PPy, GO and GF) electrodes. Graphene has fascinated marvelous interest due to their unique properties. The exhibited maximum power density by use of the globular PPy/GO/GF modified anode electrode in MFC was 1326 mW m^{-2} [41]. Furthermore, the iron-

nitrogen-functionalized graphene (Fe-N-G) composite have much better power density value (1149.8 mW m^{-2}) than pristine graphene (P-G) (109 mW m^{-2}) catalyst. The reported results that the Fe-N-G catalyst preparation method was simple and being alternative low cost electrode catalyst for MFC application [42]. Both manganese dioxide (MnO_2) and graphene nanosheets (GNS) (MnO_2/GNS) hybrid have been used in MFC application. For electrode build from GNS the air cathode catalyst generated maximum power density of 2083 mW m^{-2}, whereas for unmodified pure MnO_2 exhibited power density value of 1470 mW m^{-2} [43]. The use of graphene/PANI and carbon cloth as electrode catalyst in MFCs has been suggested by Yang and his co-workers [44].

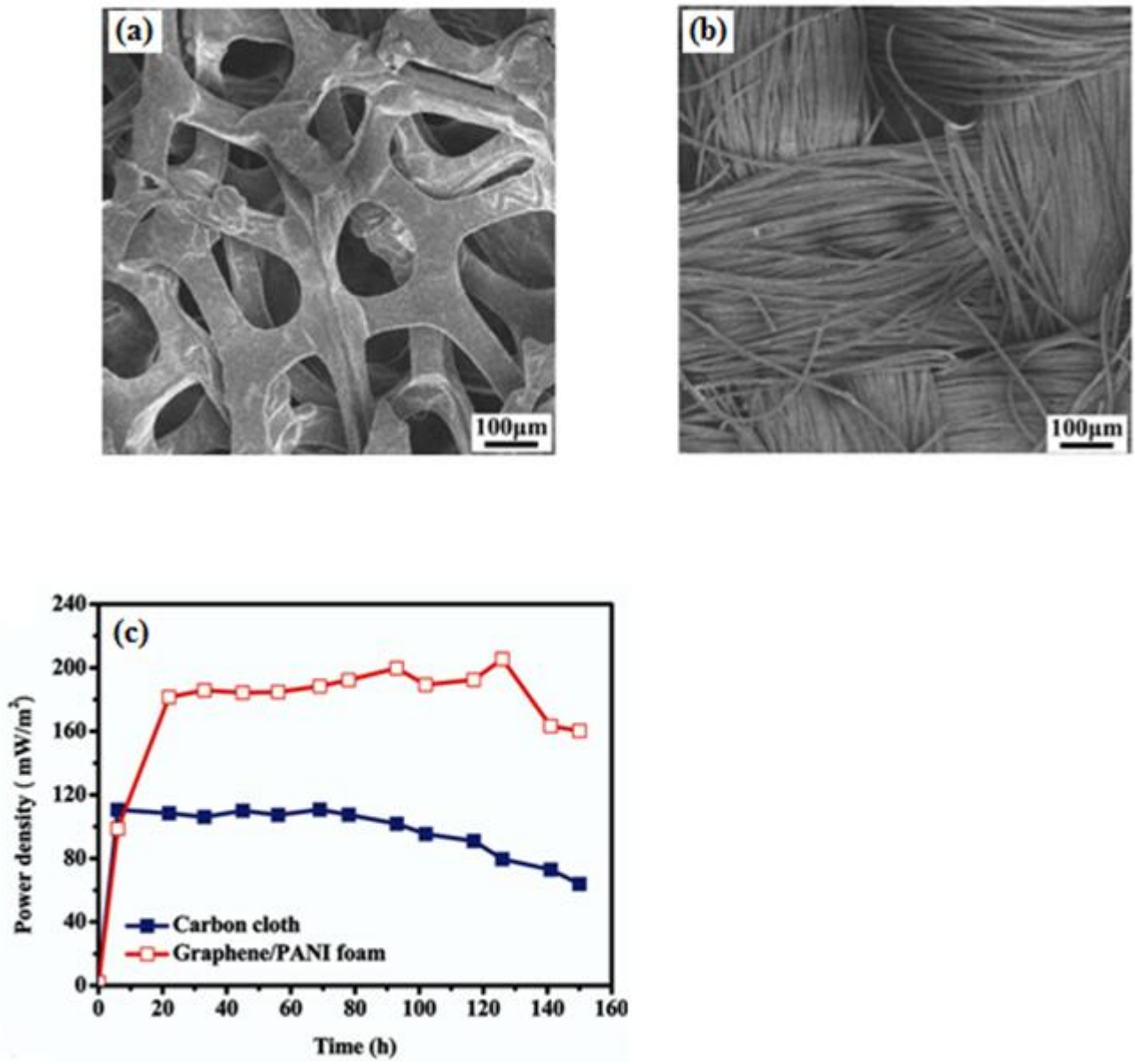

Figure 3. SEM images of (a) graphene/PANI (b) Carbon cloth (c) Time courses of the power density output of the MFCs equipped with a carbon cloth anode or a graphene/PANI foam anode. ("Reprinted with permission from (*ACS Nano* 6 (2012) 2394-2400). Copyright (2012) American Chemical Society").

Fig. 3(a) & (b) shows the SEM images graphene/PANI and carbon cloth. The parallel power performance tests have been optimized into two electrode catalysts (graphene/PANI and carbon cloth). The MFC equipped carbon cloth exhibits ~110 mW m^{-2} for 6 h, besides a 3D graphene/PANI composite reported maximum power density (~190 mW m^{-2}) for 24 hrs as shown in Fig.3c.

2.4. Metal oxide

A polycrystalline cobalt oxide modified with nitrogen doped graphene (Co_3O_4/N-G) nanocomposite proved to be capable of showing enhanced electrochemical performance in MFC energy storage devices in Fig.4 [45].

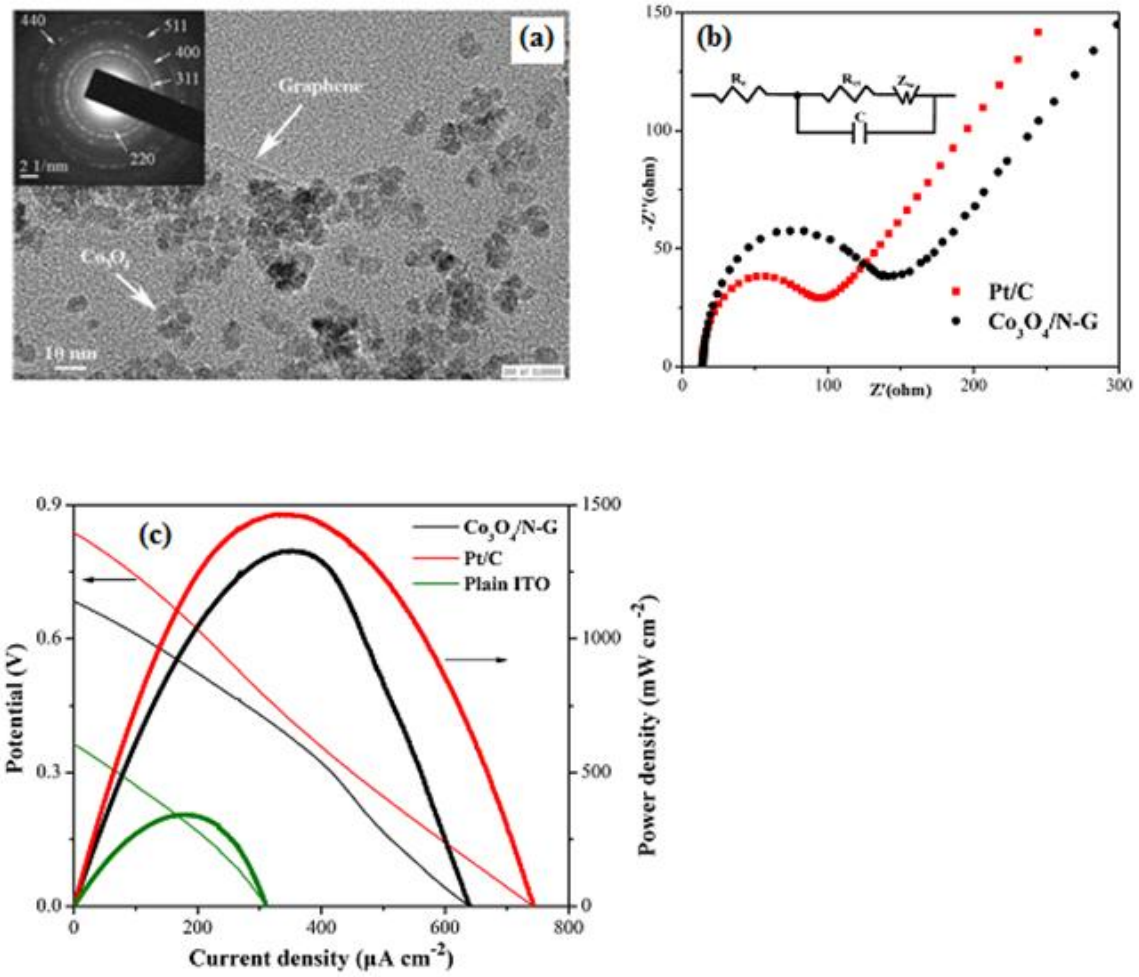

Figure 4. Transmission electron microscopy (TEM) and the corresponding selected-area electron diffraction (SAED) pattern of Co_3O_4/N-G (b) electrochemical impedance spectra of Co_3O_4/N-G and Pt/C-modified GC electrodes; inset shows the equivalent circuit of the electrochemical interface. (c) Polarization curves (thin line) and power density curve (bold line) of MFC with cathode catalysts of Co_3O_4/N-G and Pt/C and without catalyst. ("Reprinted with permission from (*Ind. Eng. Chem. Res*. 52 (2013) 6076-6082). Copyright (2013) American Chemical Society").

Gong *et al* [46] have used a simple mild-template free and ammonia-evaporation-induced method also led to the formation of cobalt oxide micro particle directly deposited on stainless steel mesh (SSM) electrode. The various morphological (Dense, three-dimensional, homogeneous and highly ordered) electrode of SSM/Co_3O_4 exhibited the resultant maximum power density value of 17.8 W m^{-3}. The development of cobalt oxide has been synthesized by heating method on a metal compound and carbon black, further it can be modify with iron phthalocyanine to obtain a new C-CoO_x-FePc composite. In MFC, the C-CoO_x-FePc cathode catalyst exhibit maximum power density value (654 ± 32 mW m^{-2}), which was 37 % higher than the power density of carbon supported FePc [47]. Mohmoud *et al* [48] employed by the solid-state reaction to produce a spinal manganese cobalt oxide (Mn-CoO) cathode used as an electrode catalyst for MFC application. The applied potential (279 mV) of MnCo-oxide cathode power density of 113 mW m^{-2} and it showed good catalytic activity towards oxygen reduction in MFC. Similarly, carbon nanotube and graphene based composite materials have been used as an alternative hybrid electrode material for oxygen reduction reaction (ORR) in air-cathode fuel cell application. The authors were employed a nano carbon hybrid materials react with cobalt oxide nanocrystals grown on nitrogen doped CNT (Co_3O_4/NCNT) or nitrogen doped reduced graphene oxide (GO) (Co_3O_4/NGO). The obtained MFC catalytic effective power generation value of 469 ± 17 mW m^{-2} for Co_3O_4/NCNT and 312 ± 15 mW m^{-2} for Co_3O_4/NGO [49]. The study nearby the report on the evaluation of power density performance of the MFC equipped with MWCNTs/SnO_2 nanocomposite. The anode was prepared by chemical method and it drops cast on the electrode surface. The incorporated MWCNTs/SnO_2 anode increased the maximum power density value of 1421 mW m^{-2} [50]. The new nanocomposite (Ruthenium oxide-carbon felt) anode material was fabricated by electrodeposition method. The RuO_2/CF achieved a maximum power density of 3.08 mW m^{-2}, when used as the MFC application [51]. Peng *et al* [52] developed iron oxide coated on the activated carbon anode (AcFeM) electrode, that fabricated the transient storage capacity reached maximum value of 574.6 C m^{-2} under 20 minutes of the open circuit interval for MFC.

2.5. Conducting polymer

Traditionally conducting polymer can be used as anode materials in MFC, because of due to their large surface area and conductivity. The surface modified bud-like shape polypyrrole supported carrageenan (PPy/KC) composite had a positive impact on the ORR in MFC application. The PPy/KC anode used as an alternative potential electrode for MFC and the reported maximum power density value of 72.1 mW m^{-2} [53]. The composite of polyaniline modified ethylene diamine anode can be synthesized using monomer of aniline and ethylene diamine by chemical method. The preparation of well known composite facilitated anode electrode in MFC, the resulted power density value of 136.2 mW m^{-2} and their coulumbic efficiency value of 21.3 % [54]. Khilari *et al* [55] used a proton exchange polymer membrane separator consisting of graphene oxide (GO), poly(vinyl alcohol) (PVA) and silicotungstic acid (STA) (PVA-STA-GO) composite anode with high surface area to increase the amount of MFC, which was gained power density of 1.9 W m^{-3}. Conducting nanostructured macroporous polyaniline modified with natural loofah sponge (PANI/LSC) composite have been

employed fabricated by in situ polymerization and the electrode surface to enhance the interaction between the sponge and anode. The produced power density of the PANI/LSC was 1090 ± 72 mW m^{-2} [56]. Similarly, the other type of in situ polymerization method has been used for the fabrication of conductive polypyrrole with reduced graphene oxide (PPy/rGO) composite. In this composite is a promising alternative technology for the production of electric current and waste water treatment. The conductive polymer composite MFCs maximum exhibited power density value of 1068 mW m^{-2} and its stability performance up to 300 h [57]. Li *et al* [58] have used four different kinds of conducting polymers like polyaniline, poly(aniline-co-aminophenol), poly(aniline-co-2,4-diaminophenol) (PANDAP) and poly(aniline-1,8-diaminonaphthalene) (PANDAN) modified with carbon felt anode. Thus the composite revealed its biocompatibility and the promoted power density value of 99.7 mW m^{-2}. A simple sol-gel, hydrothermal methods have been used for the fabrication PANI/TiO_2 composite and it was further anaerobically adhered with *E.Coli* K-12.

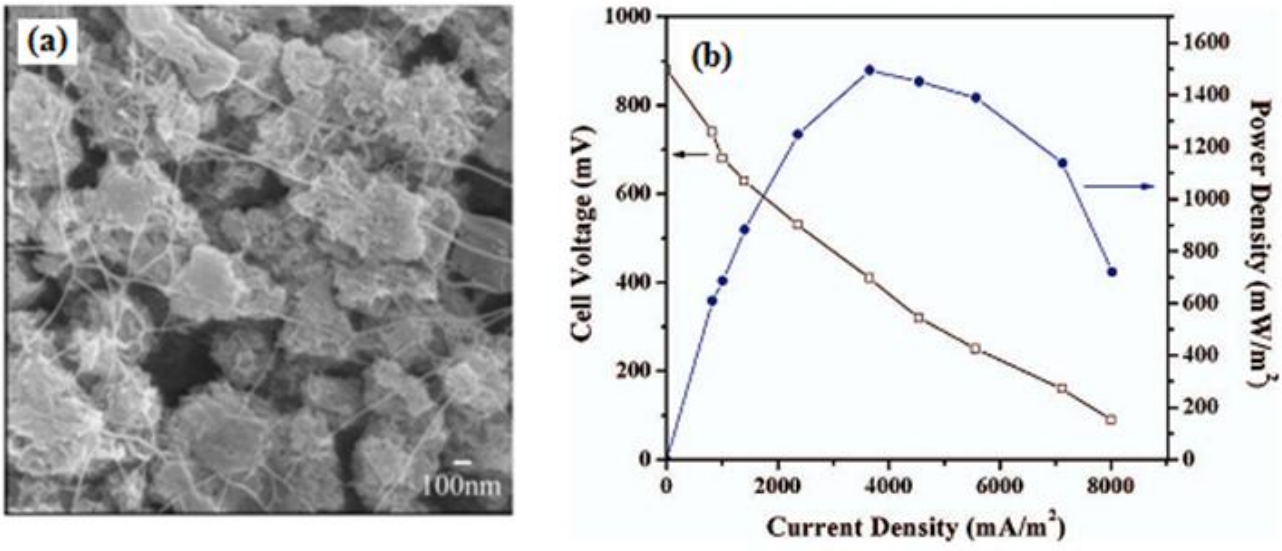

Figure 5. (a) SEM micrographs of *E.Coli* cells adhered on a 30 wt % PANI/TiO_2 electrode surface and free-floating cells (b) Power output and polarization curve of MFC with 30 wt % PANI/TiO_2 composite anode. ("Reprinted with permission from (*ACS Nano* 2 (2008) 113-119). Copyright (2008) American Chemical Society").

In Fig.5 showed the morphological and electrochemical characterization for the evaluation of power performance analysis [59].

2.6. Metal nanoparticle catalyst

Different forms of metal nanoparticles have been used for the development of MFC applications. Nickel (Ni) nanoparticle dispersed based web of carbon micro-nanofiber (ACFs/CNFs) have been prepared by chemical vapour deposition method (CVP) using *E-Coli*. The yielded power density and open circuit potential (OCP) were estimated by polarization curve and linear sweep

voltammetry methods ie 1145 ± 20 mW m^{-2} and 710 ± 5 mV respectively [60]. Palladium nanoparticle has found a special place in the field of MFC, which are great interest due to their improved properties and low surface density with uniform shape morphologies.

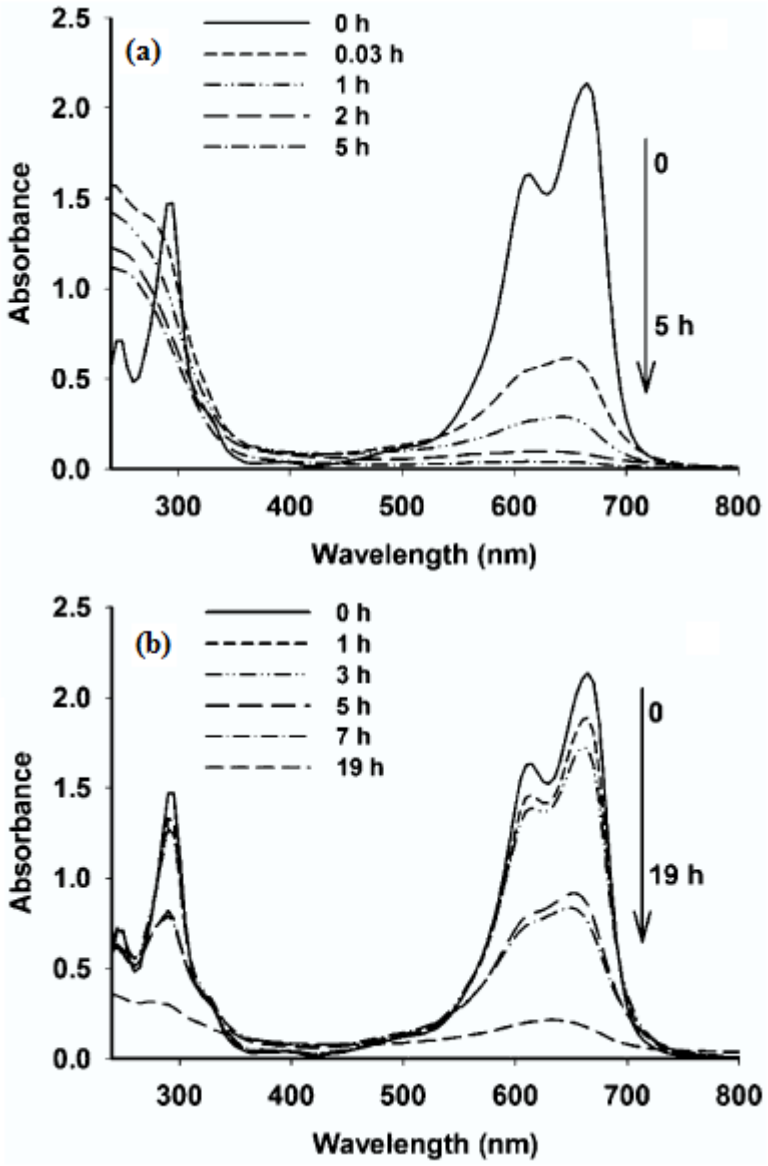

Figure 6. Absorption spectral changes of MB aqueous solution in the MFC cathode with initial addition of 0.176 mM H_2O_2 in the (a) presence and (b) absence of (+) AuNPs. Experimental conditions: 16 mg/L MB, 50 mL (+) AuNPs, pH = 3. ("Reprinted with permission from (*Ind. Eng. Chem. Res.*, 52 (2013) 8174-8181). Copyright (2013) American Chemical Society").

The new carbon supported palladium cathode electrode hold great promise as an active component in MFCs to facilitate hydrogen production. This cathode catalyst showed lower over potential value and higher columbic efficiency than the Pt catalyst [61]. The development of new catalyzed three-dimensional mesoporous anode based on stainless steel fiber felt continue to attract the keen attention in MFCs application. The modified 3D anode catalyst provided large surface area and it

could greatly reduce the MFCs internal resistance value. The resulted modified anode electrode delivered a maximum power density value of 2142 mW m^{-2} at the applied current density of 6.1 A m^{-2} [62]. Yang *et al* [63] has fabricated a polyamideamine (PAMAM) dendrimer encapsulated platinum nanoparticle (Pt-DENs) as a promising cathode catalyst for air-cathode single chamber microbial fuel cell (SCMFCs) studies by template method. The assembled uniform diameter distributed Pt-DENs catalyst, which was the reported power density value of 630 ± 5 mW m^{-2} at 5200 ± 10 mA m^{-2}. Ghasemi *et al* [64] studied four different electrode catalysts (Carbon black, nickel nanoparticle (Ni)/C, phthalocyanine/C and copper-phthalocyanine/C) were used in MFC analysis. These electrodes have been tested by cyclic voltammetry and linear sweep voltammetry, the reported maximum power density and columbic efficiency were achieved by copper-phthalocyanine/C at 118.2 mW m^{-2} and 29.3 %. A gold and cobalt oxide entrenched polypropylene-g-polyethyleneglycol catalyst has been extensively evaluated for enzymatic renewable fuel cell applications. By using 10 mM glucose, the optimized enzymatic fuel cell (EFC) generated power density value of 14 μW cm^{-2} [65]. The detailed spectral absorption investigation of methylene blue (MB) on positively charged gold nanoparticles [(+) AuNPs] by UV-visible spectroscopy (Fig.5). The observed MFC power generation was 35.5 and 20.56 mW m^{-2} in the presence and absence of (+) AuNPs [66].

2.7. Bimetallic nanoparticle

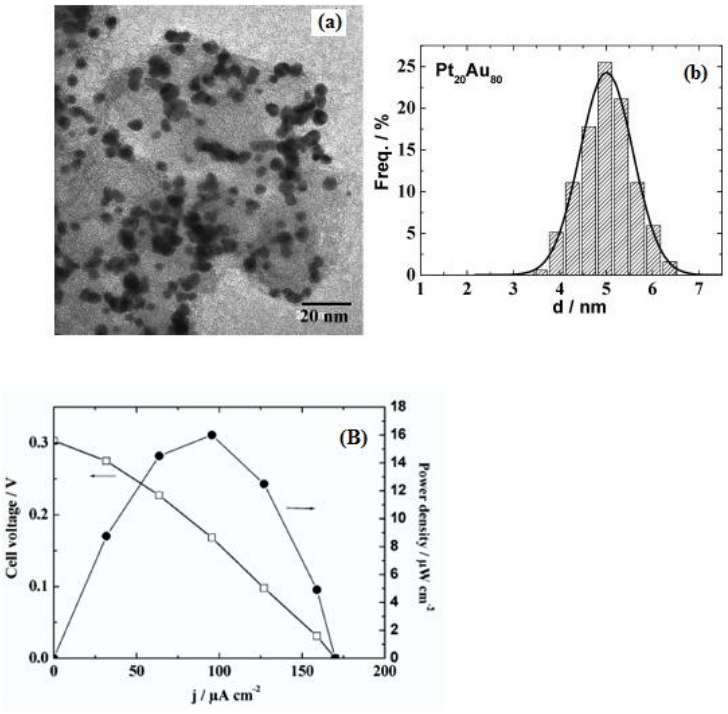

Figure 7. (A) TEM image (a) and histogram of particle size distribution (b), deduced from TEM image. $Pt_{20}Au_{80}$/C catalyst synthesized by w/o emulsion. (B) Performance of glucose/O_2 fuel cell using $Pt_{20}Au_{80}$ anode and bio-cathode (ABTS + Laccase 27 mU cm^{-2}) in phosphate buffer (pH = 5.0) at 37 °C. (a) Cell voltage *vs* current density; (b) power density vs current density. ("Reprinted with permission from (*J. Phys. Chem*. B 111 (2007) 10329-10333). Copyright (2007) American Chemical Society").

The oxygen reduction reaction (ORR) properties of a wide variety of Pt-Pd alloy electrode was exploited in the fabrication on the carbon paper electrode by electro-deposition method. The interest in Pt-Pd alloy displayed good ORR activity, after the 15^{th} cycle deposition of Pt-Pd cathode showed the maximum power density value of 1274 mW m^{-2} [67].

A facile and efficient method of Pt_xFe nanoparticles have been synthesized by $NaBH_4$ reduction (Room temperature) method. The high and homogeneous dispersion of spherical nanoparticle of Pt_xFe NPs were highly dispersed on carbon supported materials, the average particle size value of 2 nm. The cathode catalyst has been optimized through cyclic voltammetry and linear sweep voltammetry, the maximum obtained power density value of 1680 ± 15 mW m^{-2}, which was produced from MFC with Pt3-Fe/C catalyst [68]. Among these alloys, alumina (AA) and nickel (Ni) nanoparticle dispersed multi-scale of carbon micro nanofibers (ACFs/CNFs) electrode is a very fashionable material because of its power performance and electrode stability in MFC. Also, the fabricated AA:Ni-ACF/CNF catalyst showed an optimized open circuit potential value of ~0.9 V and its power density value of 1780 mW m^{-2} [69]. Novel water, oil micro emulsion procedure for the preparation of platinum-gold (Pt-Au) alloy was reported. In order to the estimated dispersion mean particle size distribution diameter of 5.0 ± 0.56 nm (Fig.7.a&b). The cell-voltage curve (Fig.7.c) was obtained the maximum power performance value occur at 0.16 V vs RHE [70].

2.8. Composites

Khilari *et al* [71] demonstrated a possibility for the analysis of proton conducting membrane in single-chambered MFC (sMFC). The as-prepared graphene oxide impregnated poly(vinyl alcohol) and silicotungstic acid (PVA-STA-GO) composite exhibits better kinetic properties, longer durability and the reported power density value of 1.9 W m^{-3} (Fig.8). Novel Fe_3O_4/CNT nanocomposites were used as an anode electrode material for MFC and it was prepared by Solvo-thermal method. By the modified 30 wt% of Fe_3O_4/CNT anode exhibited power density value of 830 mW m^{-2} and the Nyquist plot showed the smallest semi-circle region occur at a very low R_{CT} value [72]. Although, in situ chemical polymerization of pyrrole modified with CNT (PPy/CNT) composite act as an anode with *E.Coli* act as a biocatalyst. The tubular morphology of PPy-CNT composite delivered the best power performance output of 228 mW m^{-2} [73].

Meanwhile, the addition of nitrogen-doped carbon nanotube (NCNT) to a Co_3O_4 (Co_3O_4/NCNT) composite catalyst as anode could also offer good prospects in MFC applications, ie the achieved power density (469 ± 17 mW m^{-2}) which was 5.3 times greater than that of NCNT cathode [74]. On the other hand, comparative study of porous nitrogen-doped carbon nanosheet (PNCN) has been used as an alternative (Pt/C) electrode catalyst for ORR in air-cathode MFC application. The high concentrated nitrogen and large surface area of PNCN exhibited excellent electrocatalytic activity ie the maximum obtained the power density value 1159.34 mW m^{-2}, which was higher than that of Pt/C (858.49 mW m^{-2}) electrode [75].

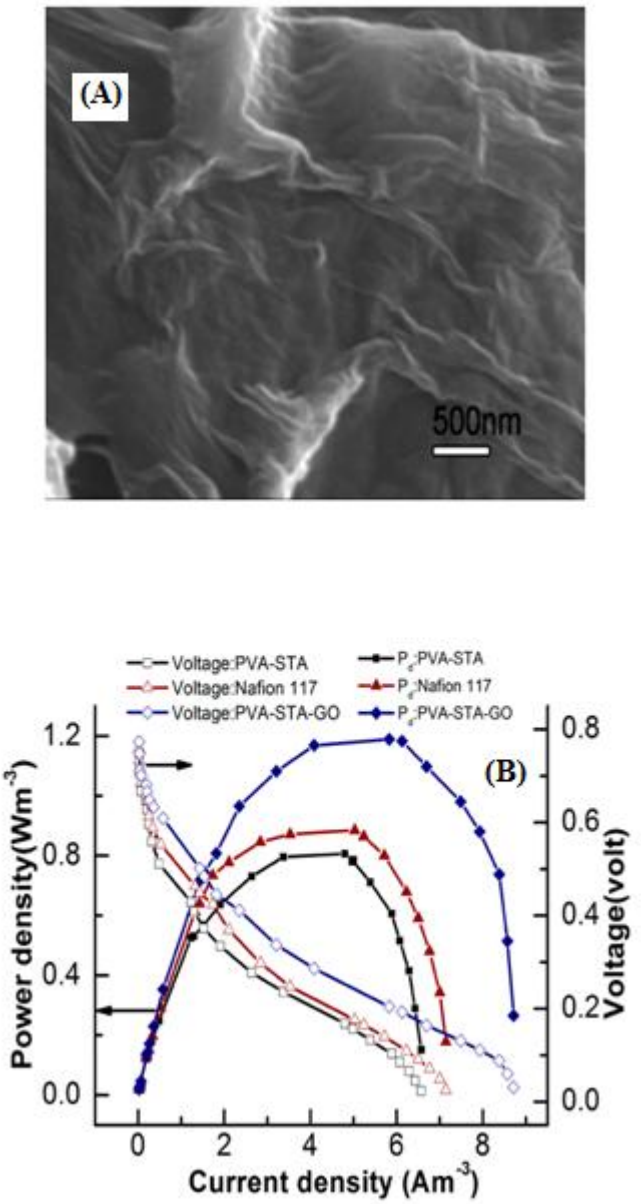

Figure 8. (A) Cross-sectional SEM images of PVA−STA−GO membranes. (B) Comparison of polarization results for MFCs using Nafion 117, PVA−STA, and PVA−STA−GO membranes. ("Reprinted with permission from (*Ind. Eng. Chem. Res* 52 (2013) 11597-11606). Copyright (2013) American Chemical Society").

Lim *et al* [76] used custom-made a proton exchange membrane (PEM) incorporated with sulfonated poly(ether ketone) (SPEEK) in poly(ether sulfonate) composite membrane. This type of membrane (PEM/SPEEK) has been characterized by the following parameters like, roughness, proton conductivity, oxygen reduction, water cross over and electrochemical impedance. Addition (5 %) of SPEEK on PES membrane, the EIS showed during the MFC analysis, the conductance and capacitance were greatly reduced from 6.15 x 10^{-7} to 6.93 x 10^{-5} and from 3.00 x 10^{-7} to 1.56 x 10^{-3} F respectively. Sadrabadi *et al* [77] has fabricated a sulfonated poly(ether ether ketone) and montmorillonite (SPEEK-70/MMT) nanocomposite for air-breathing MFCs. The optimized 3 wt % of SPEEK-70/MMT-3

membrane exhibit considerably higher open circuit potential (OCV) value and the optimized power density value of 68 mW cm^{-2} occur at 720 mA cm^{-2}. A dual chamber of two common and two shelf-fabricated proton exchange membrane of Nafion 112 & Nafion 117, which were compared to SPEEK and Cloiste 15A clay (CC)/2,4,6-triaminopyrimidine (TAP) nanocomposite for power generation and waste water treatment in MFC analysis. The chemical oxy demand (COD) (5000 mg/l) of Nafion 117 reached a higher power density (324.7 mW m^{-2}) than the others [78]. Wu *et al* [79] used a three-dimensional carbon nanotube-gold-titania (CNT/Au/TiO_2) nanocomposite used as anode catalyst for MFCs. The MFC equipped with CNT/Au/TiO_2 nanocomposite could provide enhanced stability, high electricity production efficiency and the delivered maximum power density value of 2.4 mW m^{-2}.

2.9. Bio-cathode

Zhang *et al* [80] reported that a three-dimensional graphene networks (3D-GNs) substrate was immobilized of laccase (Lac) and dopamine (DA) in glucose/O_2 bio-fuel cell applications. The fabricated Nafion/Lac/3D-GNs-PTCA-DA/GCE cathode and Nafion/glucose oxidase/ferrocene/3D-GNs/GCE anode were reported the output power density of 112 μW m^{-2} at the applied current density value of 0.96 mA cm^{-2}. Another application involves the use of carbon nanodots (CNDs) entrapped with glucose oxidase (GOx) and bilirubin oxidase (BOD) in direct electron transfer (DET) in bio-fuel cell. The CNDs/GOx/BOD catalyst has found a special place in the field of bio-fuel cell application, the displayed open-circuit voltage (OCV) value of 0.93V and the obtained power density value of 40.8 μW m^{-2} at 0.41V [81]. The enzyme based bio-fuel cell (EFCs) can be modified deoxyribonucleic acid-wrapped with single-walled carbon nanotube (SWCNT) composite electrode of great interest due to their improved the active site onto oxidized modified electrode. The modified DNA-wrapped SWCNT and GOD electrode hold great promise component of the active site increased stability of GOD in serum ie the enabled power production value of 190 μW m^{-2} up to one week duration [82]. Strik *et al* [83] used two chambers MFC with an anode and cathode. The bio-cathode was made up of cation exchange membrane and graphite felt used as a cathode. The investigated cathodic bio-electrode were exhibited the power density value of 3.1 mW m^{-2} with a 384Ω, similarly the anodic bio-cathode achieved the maximum power density value of 41 mW m^{-2} with a 102 Ω internal resistance. A bio-fuel cell (BFC) used a wide range of cellulose modified MWCNT and it was operated under buffer medium. The power output of BFC studies, the applied open circuit voltage value of 0.61V and its corresponding potential difference of both bio-cathode and anode. The maximum generated power output value of 7.9 μW at their respective current of 14.2 μA [84].

3. EFFECT OF PARAMETERS

3.1. Effect of pH

Electrolyte of pH is one of the important parameters to optimize their electrocatalytic activities. He *et al* [85] have used an air-cathode MFC with mixed bacterial culture at different pH (8 to 10)

electrolytic conditions. The optimized peak current was grouped into two stages. Such as, an increasing the current generation between pH 5 and 7 ie the reaction rate of both anodic and cathodic reactions takes place. In the second case, when the electric current increase between pH 7 and 10 resulted the decrease of R_p^c and R_p^a increase from 578 to 1855 Ω. Finally, air-cathode MFC exhibit good optimal conditions between pH 8 and 10, while the polarization resistance curve decreased with increasing pH and it improved the electrocatalytic reaction. Wang *et al* [86] also found that, activated carbon (AC) used as an air-cathode material in MFC applications. The AC cathode MFC in both acidic and alkaline conditions, the enhanced power density (804 ± 70 mW m^{-2}) was obtained from alkaline medium than acidic pre-treatment decreased the power (537 ± 36 mW m^{-2}) output. A tubular air-cathode of two-chamber MFCs have been allowed to the adjustment of higher anodic (pH = 10) and lower cathodic (pH = 2.0) supporting electrolyte solution. In an anode (pH = 10) catalyst contributed a significant enhancement of coulombic efficiency and the obtained maximum power density value of 29.9 W m^{-3} [87]. Nanocrystalline carbon-supported silver/tungsten carbide (Ag-WC/C) composite has been synthesized by hydrothermal method. The synthesized homogeneous average particle diameter of 14 nm, it can be used as a platinum-free high efficiency catalyst and cost-effective ORR electrocatalysis biomass in MFC. Ag-WC/C nanohybride showed high electrocatalytic activity under neutral conditions and the achieved four-electron transfer in ORR [88]. Nimje *et al* [89] used a culture of pure Enterobacter cloacae to produce power generation in MFC applications with carbon supported double-chamber catalyst. The catalyst was studied with wastewater by adjusting the various supporting electrolytic conditions (pH = 6.5 and 9.5). The optimized polarization curve operated under pH = 7.4 and the obtained high performance power density value of 0.0042 mW cm^{-2}. The other type of carbon cloth based dual-chamber MFC for the study of riboflavin synthesized by Shewanella operated at different pH conditions. The maximum output of electricity showed at pH = 9 under alkaline conditions, which was 1.5 times higher power output than that of neutral (pH = 7) conditions [90]. Puig *et al* [91] demonstrated that the effect of pH on induced the electricity production by used thinner graphite electrode act as an air-cathode. The increasing of pH (9.5) was directly influenced by the production of high power density (1.8 W m^{-3}) value.

3.2. Effect of temperature

Temperature is one of the important parameters for the study of microorganism in anodic biofilms of MFC. In this type of anodic bio-films were enriched with Psychrophilus bacteria Simplicispira psychrophila LMG 5408 (T) [AFO78755] and Geobacter Psychrophilus P35 (T) [AY653549]. These kinds of enriched anodic biofilms have been optimized at two different (25° C for A and 15° C for B) temperatures. The optimized polarization resistances of anode A were 177 Ω for 25° C and 82 Ω for 15° C. Hence, low optimized temperature anodic film (A) delivered lower resistance value and higher electrical conductance than B [92]. Cata *et al* [93] have used a carbon source mixture of D-glucose, D-galactose, D-xylose, D-glucuronic acid were mixed with single bacterial culture in single-chamber air-cathode mediator less catalyst occurs at different annealed temperatures (30° C and ambient-temperature). The thermally optimized (30° C and 14° C) enriched

anodic bio-film reported the maximum power density value of 486 ± 68 mW m^{-2} to 602 ± 38 mW m^{-2} at 0.31 mA cm^{-2} to 0.41 mA cm^{-2}. For the MFC study of graphite cathode electrode has been performed in power generation under the optimization of pH and temperature.

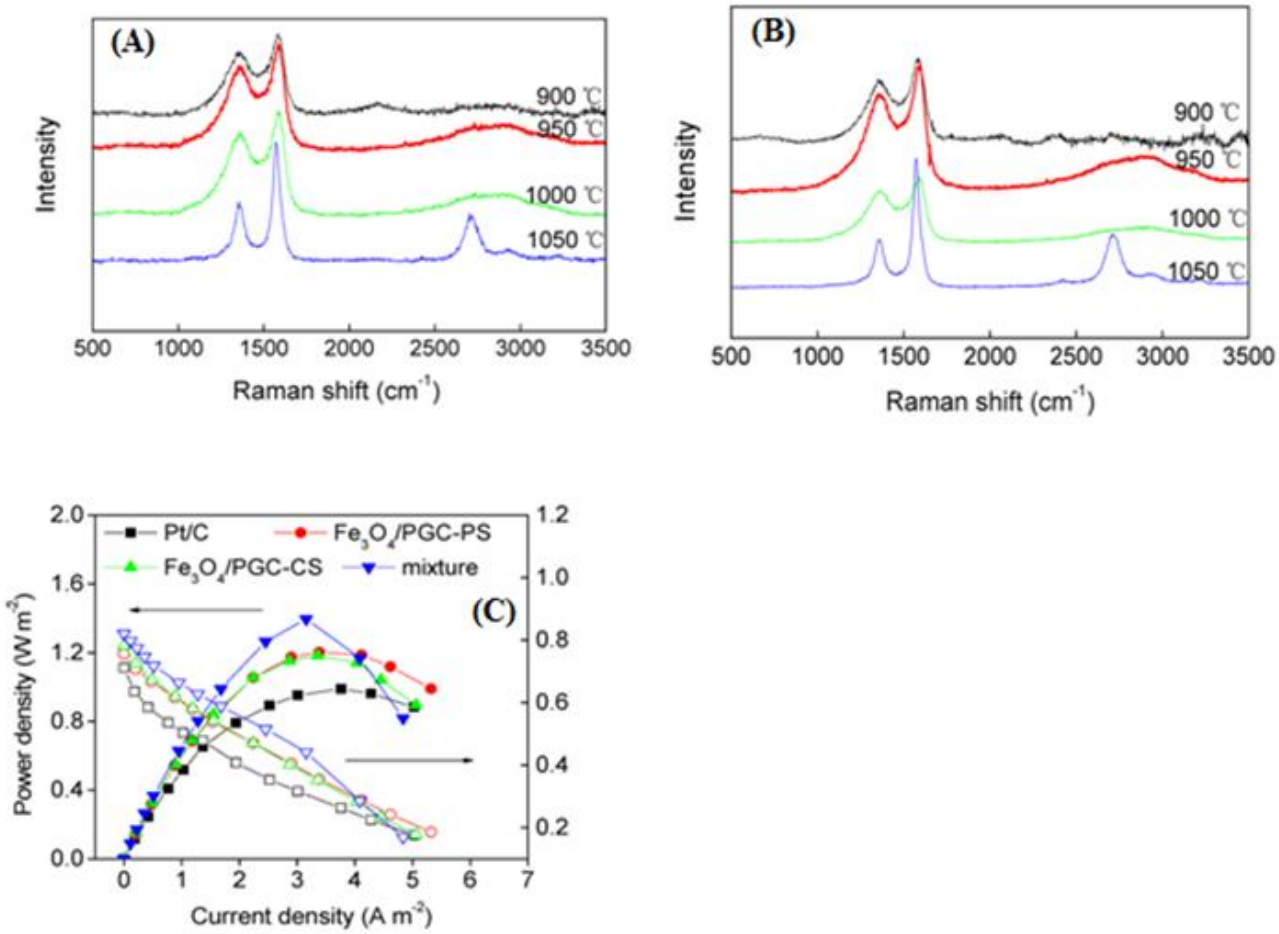

Figure 9. Raman spectrum of Fe_3O_4/PGC-CS (a) and Fe_3O_4/PGCPS (b) carbonized at 900−1050 °C. (c) Power density and the corresponding electrode potentials using different cathodes as a function of the current density at the 18th cycle the cathodes include Pt/C, Fe_3O_4/PGC-PS, Fe_3O_4/PGC-CS, and a mixture of the two composites. ("Reprinted with permission from (*ACS Appl. Mater. Interfaces* 6 (2014) 13438-13447). Copyright (2014) American Chemical Society").

The catalytic performance of graphitic electrode was evaluated to temperature variation method, as per ambient temperature variation of 20-30° C and 8-22° C. The achieved result indicated lower operating temperature favor for production of higher current and columbic efficiency than higher temperature [94]. Cheng *et al* [95] examined the practical application of MFC study of ammonia treated graphite fiber brush coated anode for waste water treatment. In MFC analysis, the operating temperature (15° C) was influenced and reproducible for the obtained power generation. Mainly, power densities were directly proportional to the temperature, but columbic efficiency was inversely proportional to the temperature. The anode and cathode were consisted into two plexiglass bottles for two chambered MFC application. The power performance study of MFC was optimized under

different thermal conditions like 40, 35, 25, 20 and 15° C. The maximum power generation was obtained under the optimal temperature of 35° C from the mixed culture [96]. Day-night temperatures (18 & 30° C) have been estimated for the performance of single-MFCs. At 6/18° C exhibit a steady-state voltage of 0.41 ± 0.005 V from 6° C and 0.36 ± 0.04 V for 18° C. The demonstrated 18/30° C exhibit higher power density (2169 ± 82 mW m^{-2}) value adopted for day-night temperature conditions [97]. Ma *et al* [98] investigated the MFC on two different iron oxide-partly graphitized carbon based (Fe_3O_4/PGC-CS and Fe_3O_4/PGC/PS) composites and they were synthesized by a simple in situ simultaneous method. The electrodes were characterized by Raman spectra at different annealed temperatures, such as 900, 950, 1000 and 1050° C (Fig.9.A and B). These kinds of electrodes were exhibited highest power density values (Fig.9.C).

4. TECHNIQUES FOR MFCS

4.1. Electrochemical impedance spectroscopic analysis (EIS)

Commercially, phthalocyanine (FePc) modified carbon black on to glassy carbon electrode by drop-casting suspension method. Carbon black/FePc composite exhibit lower over potential (~160 and ~270 mV) values and lower charge-transfer resistance value than the unmodified electrode. The cathode modified MFC exploit with Enterobacter Cloacae, it provide greater power density (400%). Similarly, beer, brewery waste water able to generate the surface yielded permissible power density (40%) values [99]. The most interesting of bundle-like morphologies of $TiO_{2(rutile)}$-$C_{(semi\text{-}graphitic)}$/$C_{(semi\text{-}graphitic)}$ nanofiber composite has been used in MFCs studies. From the Nyquist plot, the electrochemical behaviour of dual nanofiber TiO_2 based composite showed better electrocatalytic performance and very low resistance (3.149 Ω) value [100]. Zhang *et al* [101] have used three-different bio-cathode electrode materials (Graphite felt (GF), carbon paper (CP) and stainless steel mesh (SSM)) were commonly used in an MFC application. The most beneficial application of biocathodes has been tested by cyclic voltammetry, power generation, polarization and EIS analysis. The long term (50 days) stability study has been estimated by EIS technique; R_{CT} of GF-biocathode exhibited ~11 Ω than CP-biocathode (~23 Ω) and SSM-biocathode (~820 Ω). The resulted GF-bio-cathode was one of the most suitable electrode catalysts for MFC analysis. A novel use of naturally occurring plant electrode materials (King mushroom, wild mushroom and corn sterm) has been used as biofilm electrode of MFC. The following electrochemical and bioelectrochemical techniques have been used to optimize the electron transfer rate (K_{app}), charge transfer resistance and current density values etc. The standard Fe^{2+}/Fe^{3+} redox system resulted, the electron transfer resistance (R_{CT}) value 94 Ω for carbonized corn stem electrode catalyst and the maximum obtained bio-catalytic current density (i_{Max}) value of 3.12 mA cm^{-2}. The main objective of the porous architecture, natural carbon anode, which can be used as a novel and low-cost alternative materials for MFC [102]. Kumar *et al* [103] have developed by the enrichments of electrode catalyst. The intention of this study a chemical (C, terminal electron acceptor Fe(III)), electrochemical (E) and hybrid (H) methods has been fabricating a saline-solidic soil inculum. The observed 'C' enriched method delivered superior power density value (Pan, max = 49 mW m^{-2})

and the lower resistance value (1632 Ω) by EIS. Particularly for the study of MFC, gold electrode was used anode catalyst for the power generation from waste water and acetate wastewater. The achieved maximum power density (6.58 W m^{-2}) value has been measured R_{int} by EIS [104]. Similarly, gold nanoparticles (AuNPs) can be modified on the carbon paper electrode by layer-by-layer (LBL) method. The modifier anode exhibited better electrochemical behavior. The MFC of Au NP/CP achieved reasonable power density (346 mW m^{-2}) and its durability (170 h) of the chemical reaction [105].

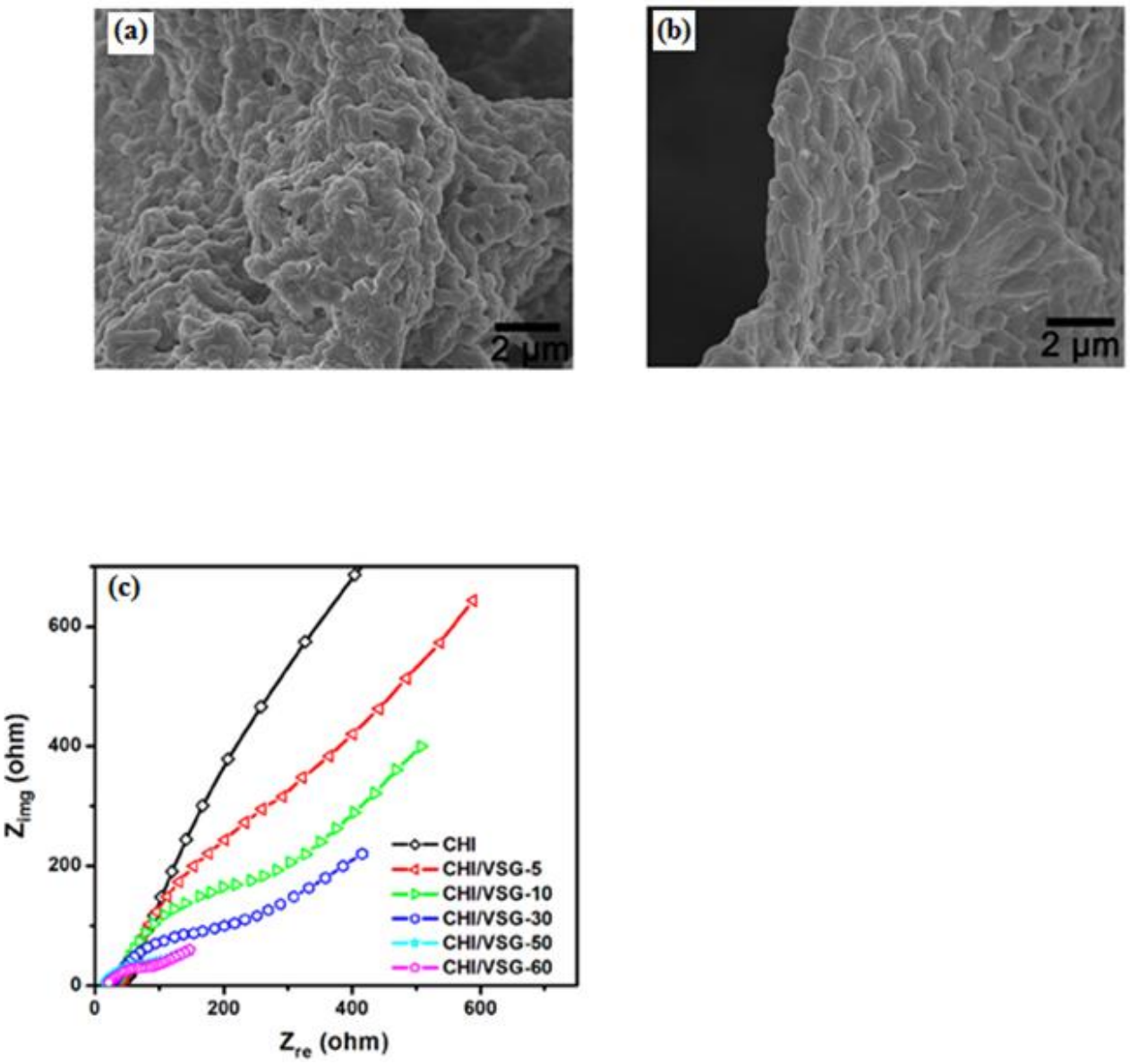

Figure 10. SEM images of CHI/VSG-50 (a) and CHI/RGO-50 (b) scaffolds after incubation with bacteria (c) Nyquist plots of different CHI/VSG electrodes. ("Reprinted with permission from (*Nano Lett.*, 12 (2012) 4738-4741). Copyright (2012) American Chemical Society").

The electroactivity of a biocompatible chistosan and vacuum-stripped graphene-50 (CHI/VSC-50) composite incubated with P.aeruginosa towards MFC was studied using EIS in Fig.10. The remarkable hierarchical pores and unique VSG cathode achieved the highest power density [106].

4.2. Cyclic voltammetry

Our selected electrodes were fabricated of an electrode material showed a symmetrical response in the cyclic voltammetry method. Use of pre-fermentation food waste (PFW) composite has been used as an anodic electrode for the production of bioelectricity in a single chamber MFC method. Cyclic voltammetry helps, PFW catalyst showed a significant power improvement after the pre-fermentation (530 mA m^{-2}) than unfermented food waste (UFW) (361 mA m^{-2}) material [107]. The electrochemical catalytic properties of mesoporous carbon (MC) modified on carbon paper air-cathode can be seen as a single chamber MFC application. The electrochemical properties of MC/A cathode have been evaluated by the cyclic voltammogramme method. The MC modifier electrode obtained well defined redox peak potential and the enhanced current response. The power performance curve was reported, the achieved power density value of 237 mW m^{-2} [108]. The active bacterial biofilm has been reported a conventional cyclic voltammetry method for the evaluation of electrochemical standard redox behavior in MFC. The highlighted charge-discharge curve of the bioactive electrode film was clearly visualized the in the electro active redox behavior [109]. Sharma *et al* [110] developed anoxic bio-cathode used sulphate-reduced bacteria (SRB) fabricated on activated carbon fabric (ACF) stainless steel (SS) mesh electrode. Here the improved bio-cathode power density value was observed 4.79 to 23.11 mW m^{-2} at the applied power density of 75 to 250 mA m^{-2}. The improved electric current and better redox behavior has been analyzed from the voltammetric method. A novel, inexpensive and three-dimensional structure of carbon nanotube –coated stainless steel mesh (SSM) (CNTs/SSM) bio-cathode has been used in MFC. The bio-cathode was characterized by the cyclic voltammetry method, the abiotic CNT-SSM electrode exhibited higher power density (147 mW m^{-2}) than the abiotic SSM (3 mW m^{-2}) electrode [111]. Sun *et al* [112] demonstrated two kinds (Electrochemical & microbial) of reaction involved in the sulfide oxidation process in MFC. The electrochemical oxidation reactions were carried out in three states in compound conditions. Such as, sulfide and S_x^{2-} exhibit the oxidative peak potential of E_p = -1.4 V, whereas $S_4O_6^{2-}$ weak peak of E_p = -0.75 V and a new species of $S_2O_3^{2-}$ obtained at -0.2 to -0.25 V. The above kinds of sulphur transformation (Sulfide oxidation) would generate electricity in a laboratory scale MFC application.

4.3. Power density

Nitrogen-doped graphene (NG) has been explored as cathode catalyst for MFC applications. NG catalyst has been synthesized by the Hummer's method; the polarization curve resulted in the power density values of NG-MFCs and Pt/C-MFCs. Here NG-MFCs generated power density value of 776 ± 12 mW m^{-2}, whereas Pt/C-MFCs exhibit 750 ± 19 mW m^{-2} [113]. The nano tubular MnO_2/graphene oxide composite has been prepared by a simple and efficient hydrothermal method. *α*-

MnO_2 exhibit efficient catalytic activity toward ORR, the maximum power density value (3359 mW m^{-2}) of MnO_2/graphene oxide composite, which was 7.8 times higher than that of unmodified electrode [114]. Xia *et al* [115] have used two-chamber electrode, the air-cathode MFC of biocathode exhibited the power density value of 554 ± 0 mW m^{-2}, which was the comparable obtained Pt electrode (576 ± 16 mW m^{-2}) value. There has been an interesting report on the hydrothermal preparation of the crystalline spinal structure of cobaltosic and nitrogen-doped graphene (Co_3O_4/N-G) nanocomposite cathode. Very flexible and tough nanocomposite could be obtained the electrochemical measurement of power density value 1340 ± 10 mW m^{-2} obtained at the applied open-circuit voltage value of 0.68 ± 0.05 V. This composite power density value, which was four times (340 ± 10 mW m^{-2}) higher than that of plain cathode [116]. To improve the ORR, a cost-effective and long durability of activated carbon (AC) powder was paralyzed with iron ethylenediaminetetraacetic acid (FeEDTA) (0.2:1 ratio) on the stainless steel mesh electrode. The pyralized based catalyst has been commonly used as MFC studies, the collector produced power density value of 1580 ± 80 mW m^{-2} than the plain AC (1440 ± 60 mW m^{-2}) cathode. In this powerful performance was mainly due to the electrode specific surface area of FeEDTA-AC (810 ± 5 m^2 g^{-1}), which was 8 % lower (883 ± 5 m^2 g^{-1}) value than unmodified AC cathode [117]. Recently, the use of unique 3D vertically oriented TiO_2 nanosheets (TiO_2-NSs) was synthesized by *in situ* method on the carbon paper (CP) electrode. This study was carried out using cyclic voltammetry and electrochemical impedance spectroscopy methods. It was shown that the maximum power output density of TiO_2-NSs/CP bio-anode exhibited 690 mW m^{-3}, this was increased relative to that of 423 mW m^{-3} for bare CP electrode [118]. In another related study, electrodeposition technique was used to study the novel conductive carbon nanotube (CNT) hydrogel and chistosan onto a carbon paper electrode. The power performance study has been used in two different of anode electrode materials in MFC. Hereafter, CNT hydrogel modified electrode power density value of 132 mW m^{-2} [119].

4.4. Cell voltage study

The reduced graphene oxide (*r*GO) supported polyaniline/Pt (*r*GO/PANI/Pt) nanocomposite have been explored as a cathode catalyst for MFC applications. The interfacial properties of impedance analysis, *r*GO/PANI/Pt/CC catalyst were greatly reduced to the R_{CT} value ie due to owing improved the electrical conductivity (Fig.11a).

Similarly, the in situ polymerized and reduction method prepared *r*GO/PANI/Pt nanocomposite obtained the power density value of 2059 mW m^{-2} (Fig.11b). The electrocatalytic stability of *r*GO/PANI/Pt composite voltage-time curve of MFC exhibited a rapid start up for the charge process and lower degradation of the discharged process (High stability). On the other hand, the unmodified CC electrode was exhibited faster degradation due to attain lower stability (Fig.11c) [120]. Liu *et al* [121] proposed a vertical substrate flow constructed wetland-MFC (CW-MFC) act as a bio-cathode materials. The bio-cathode catalyst commonly used three different types, such as stainless steel mesh (SSM), carbon cloth (CC) and granular activated carbon (GAC). Mainly, GAC-SSM bio-cathode attains maximum power density value of 55.05 mW m^{-2}. In this cell-voltage (day-night) study of the

profiles surface temperature and the cell voltage different CW-MFC up to 10-13 days. While GAC-SSM bio-cathode temperature fluctuation was occurring in the range between 20º C to 22º C. The effect of MFCs, Pt-carbon coated cathode and generation of increasing the power output (0.097 mW) in dissolved oxygen within 120 h after the inoculation. The stability of power generation after a long period 50 h after the inoculation of anode catalyst.

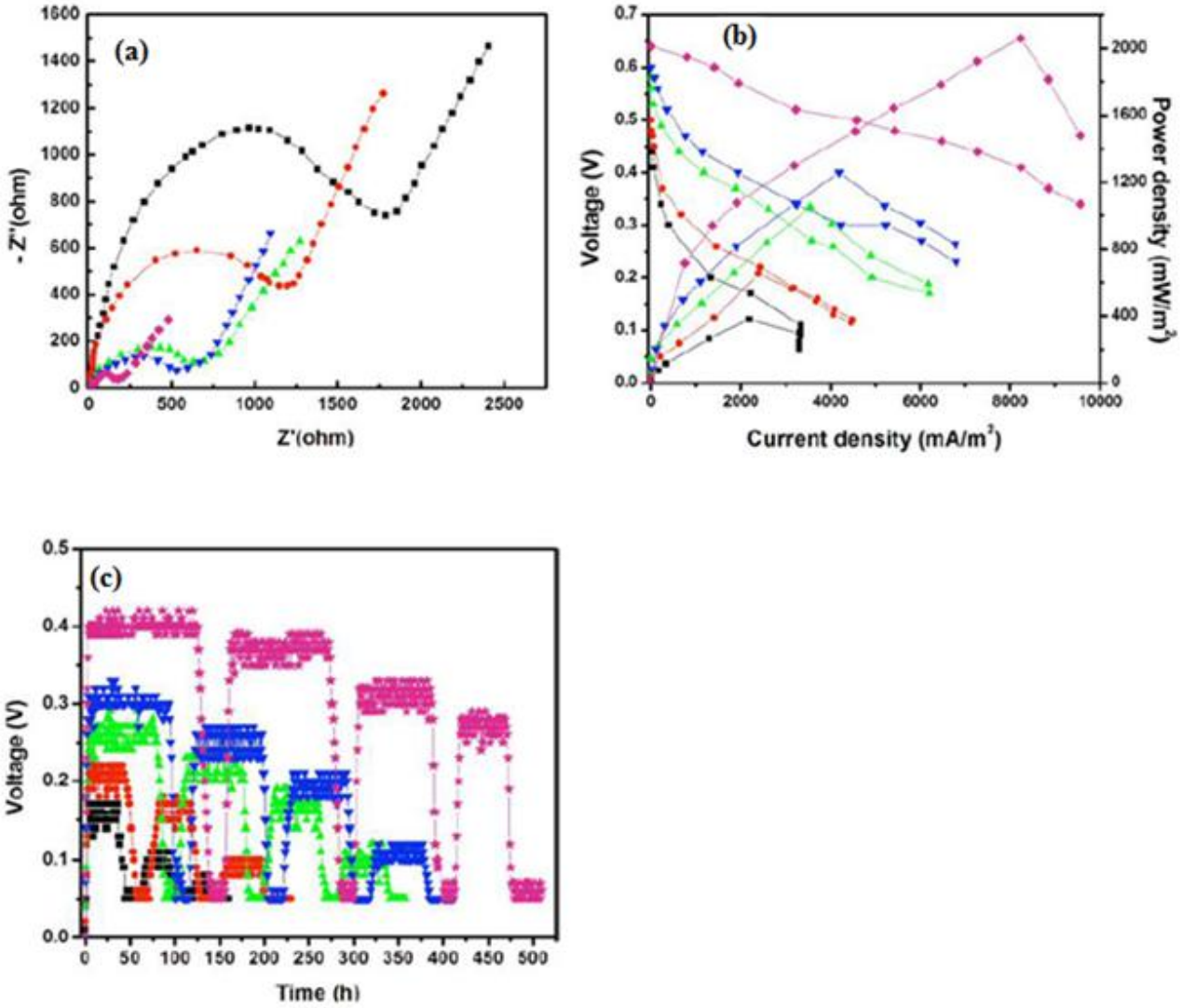

Figure 11. (a) Impedance spectra of (■) bare CC, (●) rGO/CC, (▲) rGO/PANI/CC, (▼) rGO/Pt/CC, and (♦) rGO/PANI/Pt/CC obtained under *E-Coli*, HNQ, and glucose (b) Fuel cell performances of MFC equipped with (■) bare CC, (●) rGO/CC, (▲) rGO/PANI/CC, (▼) rGO/Pt/CC, and (♦) rGO/PANI/Pt/CC. (c) Representative cell voltage−time profile of MFC equipped with (■) bare CC, (●) rGO/CC, (▲) rGO/PANI/CC, (▼) rGO/Pt/CC, and (☆) rGO/PANI/Pt/CC. ("Reprinted with permission from (*Ind. Eng. Chem. Res* 53 (2014) 16883-16893). Copyright (2014) American Chemical Society").

The optimized electrode stability cycle of voltage range (320 – 340 mV), which could rapid rise in power generation [122]. The macroporous structure of three-dimensional (3D) carbon nanotube-

textile fiber anode has been used in high performance MFC. After the 12 days long-duration operation, the operated voltage value of 0.3 V, which was across 1 kΩ resistor. This is due to clearly explain a successful start-up (stable) reaction. The highly conductive, 3D macroporous CNT-textile composite exhibit the maximum power density value (655 mW m^{-2}) obtained from the polarization curve [123]. A single-chamber of soil organic matter which can be used as an anode material attempted with MFC. The organic soil matters enriched with bacteria were mainly affiliated to *E-Coli* and Deltaproteobacteria. The resulted MFC with 5 cm deep soil and 3cm overlaying water reported the highest open circuit voltage (562 mV) and power density value of 0.72 mW m^{-2}. The cell-voltage curve exhibited a circadian oscillation that reached maximum value at afternoon and minimum value at early morning [124]. The anodic bio-film finds important application in MFC and it was developed a 100 Ω external loading of slaughterhouse waste water. The power density value determined by the polarization curve method gave a maximum high value of 578 mW m^{-2} obtained for the MFC development of 100 Ω loaded samples and the other value of 277 mW m^{-2} for the MFC developed 1 Ω loaded condition. The bio-film was optimized under 100 Ω loaded samples displayed a current-voltage signals indicated the oxidation applied potential value of -0.35 V *vs* Ag/AgCl [125].

5. CONCLUSIONS

The extensive studies of MFC catalysts play an important role in the improvement of electrode catalytic activity and long-durability. And also highlighted the most significant role of electrode properties such as particle size, morphology, active surface area and stability for their superior performance in MFC. Moreover, carbon based nanocomposite and conducting polymer based electrode catalysts were reported highest performance of electrocatalytic activities. MFC is one of the most important energy storage devices to replace the Pt based electrode catalyst for the alternative usage of bacteria (bio-cathode). Instead of MFC electrode catalyst can be used as an alternative (bio-cathode), attractive and tremendous enhancement of power output.

ACKNOWLEDGEMENT
This research work was supported by Ministry of Science and Technology, Taiwan and India-Taiwan Science and Technology Cooperation program, DST, India.

References

1. P. Zhang, K. Li, X. Liu, *J. Power Sources* 264 (2014) 248-253.
2. C. Erbay, X. Pu, W. Choi, M.J. Choi, Y. Ryu, H. Hou, F. Lin, P.D. Figueiredo, C. Yu, A. Han, *J. Power Sources* 280 (2015) 347-354.
3. V.B. Oliveira, M. Simoes, L.F. Melo, A.M.F.R. Pinto, *Biochem. Eng. J.* 73 (2013) 53-64.
4. M.H. Osman, A.A. Shah, F.C. Walsh, *Biosens. Bioelectron.* 26 (2010) 953-963.
5. S.V. Mohan, G. Velvizhi, K.V. Krishna, M.L. Babu, *Bioresour. Technol*. 165 (2014) 355-364.
6. W. Zhi, Z. Ge, Z. He, H. Zhang, *Bioresour. Technol*. 171 (2014) 461-468.
7. S. Liu, H. Song, S. Wei, F. Yang, X. Li, *Bioresour. Technol*. 166 (2014) 575-583.

8. Y. Wang, B. Li, D. Cui, X. Xiang, W. Li, *Biosens. Bioelectron*. 51 (2014) 349-355.
9. L. Xiao, J. Damien, J. Luo, H.D. Jang, J. Huang, Z. He, *J. Power Sources* 208 (2012) 187-192.
10. N. Li, Y. Liu, J. An, C. Feng, X. Wang, *J. Power Sources* 272 (2014) 895-899.
11. F. Zhao, F. Harnisch, U. Schroder, F. Scholz, P. Bogdnaff, I. Herrmann, *Electrochem. Commun*. 7 (2005) 1405-1410.
12. D.B. Wang, T.S. Song, T. Guo, Q. Zeng, J. Xie, *Int. J. Hydrogen Energy* 39 (2014) 13224-13230.
13. J. Zhang, J. Li, D. Ye, Z. Zhu, Q. Liao, B. Zhang, *Int. J. Hydrogen Energy* 39 (2014) 19148-19155.
14. V.J. Watson, C.N. Delgado, B.E. Logan, *J. Power Sources* 242 (2013) 756-761.
15. Y. Zhang, G. Mo, X. Li, J. Ye, *J. Power Sources* 197 (2012) 93-96.
16. R. Ramachandran, V. Mani, S.M. Chen, G. Gnana kumar, M. Govindasamy *Int. J. Electrochem. Sci.* 10 (2015) 859-869.
17. K.J. Babu, A. Zahoor, K.S. Nahm, R. Ramachandran, M.A.J. Rajan, G. Gnana kumar, *J. Nanopart. Res.* 16 (2014) 2250.
18. R. Ramachandran, V. Mani, S.M. Chen, R. Saraswathi, B.S. Lou, *Int. J Electrochem. Sci.* 8 (2014) 11680.
19. S.M. Chen, R. Ramachandran, V. Mani, R. Saraswathi *Int. J Electrochem. Sci.* 9 (2014) 4072.
20. R. Ramachandran, V. Mani, S.M. Chen, G. Gnana kumar, P. Gajendran, N.B. Devi, R. Devasenathipathy *Int. J Electrochem. Sci.*10 (2015) 3301-3318.
21. Q. Deng, X. Li, J. Zuo, A. Ling, B.E. Logan, *J. Power Sources* 195 (2010) 1130-1135.
22. E. Kipf, J. Koch, B. Geiger, J. Erben, K. Richter, J. Gescher, R. Zengerle, S. Kerzenmacher, *Bioresour. Technol*. 146 (2013) 386-392.
23. S. Sing, N. Verma, *Int. J. Hydrogen Energy* 40 (2015) 1145-1153.
24. J. Wei, P. Liang, X. Cao, X. Huang, *Bioresour. Technol*. 102 (2011) 10431-10435.
25. S.J. Yen, M.C. Tsai, Z.C. Wang, H.L. Peng, C.H. Tsai, T.R. Yew, *Electrochim. Acta* 108 (2013) 241-247.
26. U. Kara, E. Muto, R. Umaz, M. Kolln, C. Santoro, L. Wang, B. Li, *Int. J. Hydrogen Energy* 39 (2014) 21847-21856.
27. E. Mshoperi, R. Fogel, J. Limson, *Electrochim. Acta* 128 (2014) 311-317.
28. B. Zhang, Z. Wen, S. Ci, S. Mao, J. Chen, Z. He, *ACS Appl. Mater. Interfaces* 6 (2014) 7464-7470.
29. J.J. Sun, H.Z. Zhao, O.Z. Yang, J. Song, A. Xue, *Electrochim. Acta* 55 (2010) 3041-3047.
30. T. Sharma, A.L.M. Reddy, T.S. Chandra, S. Ramaprabhu, *Int. J. Hydrogen Energy* 33 (2008) 6749-6754.
31. Y. Zou, C. Xiang, L. Yang, L.X. Sun, F. Xu, Z. Cao, *Int. J. Hydrogen Energy* 33 (2008) 4856-4862.
32. Y. He, Z. Liu, X.H. Xing, B. Li, Y. Zhang, R. Shen, Z. Zhu, N. Duan, *Biochem. Eng. J.* 94 (2015) 39-44.
33. Y. Wu, X. Zhang, S. Li, X. Lv, Y. Chang, X. Wang, *Electrochim. Acta* 109 (2013) 328-332.
34. H.T. Chou, H.J. Lee, H.H. Tai, H.Y. Chang, *Bioresour. Technol*. 169 (2014) 532-536.
35. Y. Yuan, B. Zhao, Y. Jeon, S. Zhong, S. Zhou, S. Kim, *Bioresour. Technol*. 102 (2011) 5849-5854.
36. J.E. Mink, J.P. Rojas, B.E. Logan, M.M. Hussain, *Nano Lett*. 12 (2012) 791-795.
37. J. Hou, Z. Liu, P. Zhang, *J. Power Sources* 224 (2013) 139-144.
38. Y. Zhang, G. Mo, X. Li, W. Zhang, J. Zhang, J. Ye, *J. Power Sources* 196 (2011) 5402-5407.
39. J. Liu, Y. Qiao, C.X. Guo, S. Lim, H. Song, C.M. Li, *Bioresour. Technol*. 114 (2012) 275-280.
40. A. Mehdinia, E. Ziaei, A. Jabbari, *Int. J. Hydrogen Energy* 39 (2014) 10724-10730.
41. Z. Lv, Y. Chen, H. Wei, F. Li, Y. Hu, C. Wei, C. Feng, *Electrochim. Acta* 111 (2013) 366-373.
42. S. Li, Y. Hu, Q. Xu, J. Sun, B. Hou, Y. Zhang, *J. Power Sources* 213 (2012) 265-269.

43. Q. Wen, S. Wang, J. Yan, L. Cong, Z. Pan, Y. Ren, Z. Fan, *J. Power Sources* 216 (2012) 187-191.
44. Y.C. Yong, X.C. Dong, M.B.C. Park, H. Song, P. Chen, *ACS Nano* 6 (2012) 2394-2400.
45. Y. Su, Y. Zhu, X. Yang, J. Shen, J. Lu, X. Zhang, J. Chen, C. Li, *Ind. Eng. Chem. Res*. 52 (2013) 6076-6082.
46. X.B. Gong, S.J. You, X.H. Wang, J.N. Zhang, Y. Gan, N.Q. Ren, *Biosens. Bioelectron*. 55 (2014) 237-241.
47. J. Ahmed, Y. Yuan, L. Zhou, S. Kim, *J. Power Sources* 208 (2012) 170-175.
48. M. Mahmoud, T.A.G. Allah, K.M.E. Khatip, F.E. Gohary, *Bioresour. Technol*. 102 (2011) 10459-10464.
49. T.S. Song, D.B. Wang, H. Wang, X. Li, Y. Liang, J. Xie, *Int. J. Hydrogen Energy* 40 (2015) 3868-3874.
50. A. Mehdinia, E. Ziaei, A. Jabbari, *Electrochim. Acta* 130 (2014) 512-518.
51. Z. Lv, D. Xie, X. Yue, C. Feng, C. Wei, *J. Power Sources* 210 (2012) 26-31.
52. X. Peng, H. Yu, L. Ai, N. Li, X. Wang, *Bioresour. Technol*. 144 (2013) 689-692.
53. C. Esmaeili, M. Ghasemi, L.Y. Heng, S.H.A. Hassan, M.M. Abdi, W.R.W. Daud, H.Ilbeygi, A.F. Esmail, *Carbohydr. Polym*. 114 (2014) 253-259.
54. M. Ghasemi, W.R.W. Duad, M. Mokhtarian, A. Mayahi, M. Ismail, F. Anish, M. Sedighi, J. Alar, *Int. J. Hydrogen Energy* 38 (2013) 9525-9532.
55. S. Khilari, S. Pandit, M.M. Ghangrekar, D. Pradhan, D. Das, *Ind. Eng. Chem. Res* 52 (2013) 11597-11606.
56. Y. Yuan, S. Zhou, Y. Liu, J. Tang, *Environ. Sci. Technol*. 47 (2013) 14525-14532.
57. G. Gnana kumar, C.J. Kirubaharan, S. Udhayakumar, K. Ramachandran, C. Karthikeyan, R. Renganathan, K.S. Nahm *ACS. Sustanable Chem. Eng*. 2 (2014) 2283-2290.
58. C. Li, L. Ding, H. Cui, L. Zhang, K. Xu, H. Ren, *Bioresour. Technol*. 116 (2012) 459-465.
59. Y. Qiao, S.J. Bao, C.M. Li, Q.Q. Cui, Z.S. Lu, J. Quo, *ACS Nano* 2 (2008) 113-119.
60. S. Singh, N. Verma, *Int. J. Hydrogen Energy* 40 (2015) 1145-1153.
61. Y.X. Huang, X.W. Liu, X.F. Sun, G.P. Sheng, Y.Y. Zhang, G.M. Yan, S.G. Wang, A.W. Xu, H.Q. Yu, *Int. J. Hydrogen Energy* 36 (2011) 2773-2776.
62. J. Hou, Z. Liu, S. Yang, Y. Zhou, *J. Power Sources* 258 (2014) 204-209.
63. X. Yang, J. Lu, Y. Zhu, J. Shen, Z. Zhang, J. Zhang, C. Chen, C. Li, *J. Power Sources* 196 (2011) 10611-10615.
64. G. Ghasemi, W.R.W. Daud, M. Rahimnejad, M. Rezayi, A. Fetemi, Y. Jafri, M.R. Somalu, A. Manzour, *Int. J. Hydrogen Energy* 38 (2013) 9533-9540.
65. M.S. Kilic, S. Korkut, B. Hazer, E. Erhan, *Biosens. Bioelectron*. 61 (2014) 500-505.
66. T.H. Han, M.M. Khan, S. Kalathil, J. Lee, M.H. Cho, *Ind. Eng. Chem. Res.*, 52 (2013) 8174-8181.
67. X. Quan, Y. Mei, H. Xu, B. Sun, X. Zhang, *Electrochim. Acta* 165 (2015) 72-77.
68. Z. Yan, M. Yang, J. Liu, R. Liu, J. Zhao, *Electrochim. Acta* 141 (2014) 331-339.
69. S. Sing, N. Verma, *Int. J. Hydrogen Energy* 40 (2015) 5928-5938.
70. A. Habrioux, E. Sibert, K. Servat, W. Vogel, K.B. Kokoh, N.A. Vante, *J. Phys. Chem*. B 111 (2007) 10329-10333.
71. S. Khilari, S. Pandit, M.M. Ghangrekar, D. Pradhan, D. Das, *Ind. Eng. Chem. Res* 52 (2013) 11597-11606.
72. I.H. Park, M. Christy, P. Kim, K.S. Nahm, *Biosens. Bioelectron*. 58 (2014) 7580.
73. Y. Zhou, C. Xiang, L. Yang, L.X. Sun, F. Xu, Z. Cao, *Int. J. Hydrogen Energy* 33 (2008) 4856-4862.
74. T.S. Song, D.B. Wang, X. Li, Y. Liang, J. Xie, *Int. J. Hydrogen Energy* 40 (2015) 3868-3874.
75. Q. Wen, S. Wang, J.Y.L. Long, Y. Chen, H. Xi, *Bioelectrochemistry* 95 (2014) 23-28.

76. S.S. Lim, W.R.W. Daud, J.M. Jahim, M. Ghasemi, P.S. Chong, M. Ismail, *Int. J. Hydrogen Energy* 37 (2012) 11409-11424.
77. M.M.H. Sadrabadi, E. Dashtimoghadam, S.N.S. Eslami, G. Bahlakesh, M.A. Shokrgozar, K.I. Jacob, *Polymer* 55 (2014) 6102-6109.
78. H. Ilbeygi, M. Ghasemi, D. Emadzadeh, A.F. Ismail, S.M.J. Zaidi, S.A. Aljlil, J. Jaafar, D. Martin, S. Keshani, *Int. J. Hydrogen Energy* 40 (2015) 477-487.
79. Y. Wu, X. Zhang, S. Li, X. Lv, Y. Cheng, X. Wang, *Electrochim. Acta* 109 (2013) 328-332.
80. Y. Zhang, M. Chu, L. Yang, Y. Tan, W. Deng, M. Ma, X. Su, Q. Xie, *ACS Appl. Mater. Interfaces* 6 (2014) 12808-12814.
81. M. Zhao, Y. Gao, J. Sun, F. Gao, *Anal. Chem.* 87 (2015) 2615-2622.
82. J.Y. Lee, H.Y. Shin, S.W. Kang, C. Park, S.W. Kim, *Enzyme Microb. Technol.* 48 (2011) 80-84.
83. D.P.B.T.B. Strik, H.V.M. Hamelers, C.J.N. Buisman, *Environ. Sci. Technol*. 44 (2010) 532-537.
84. X.E. Wu, Y.Z. Guo, M.Y. Chen, X.D. Chen, *Electrochim. Acta* 98 (2013) 20-24.
85. Z. He, Y. Huang, A.K. Manoher, F. Mansfeld, *Bioelectrochemistry* 74 (2008) 78-82.
86. X. Wang, N. Gao, Q. Zhou, H. Dong, H. Yu, Y. Feng, *Bioresour. Technol*. 144 (2013) 632-636.
87. L. Zhuang, S. Zhou, Y. Li, Y. Yuan, *Bioresour. Technol*. 101 (2010) 3514-3519.
88. X.B. Gong, S.J. You, X.H. Wang, Y. Gan, R.N. Zhang, N.Q. Ren, *J. Power Sources* 225 (2013) 330-337.
89. V.R. Nimje, C.Y. Chen, C.C. Chen, J.Y. Tsai, H.R. Chen, Y.M. Huang, J.S. Jean, Y.F. Chang, R.C. Shih, *Int. J. Hydrogen Energy* 36 (2011) 11093-11101.
90. Y.C. Yong, Z. Cai, Y.Y. Yu, P. Chen, R. Jiang, B. Cao, J.Z. Sun, J.Y. Wang, H. Song, *Bioresour. Technol*. 130 (2013) 763-768.
91. S. Puig, M. Serra, M. Coma, M. Cabre, M.D. Balaguer, J. Colprim, *Bioresour. Technol*. 101 (2010) 9594-9599.
92. L. Liu, O. Tsygonova, D.J. Lee, A. Su, J.S. Chong, A. Wang, N. Ren, *Int. J. Hydrogen Energy* 37 (2012) 15792-15800.
93. T. Catal, P. Kavanagh, V.O. Flaherty, D. Leech, *J. Power Sources* 196 (2011) 2676-2681.
94. G.S. Jadhav, M.M. Ghangrekar, *Bioresour. Technol*. 100 (2009) 717-723.
95. S. Cheng, D. Xing, B.E. Logan, *Biosens. Bioelectron*. 26 (2011) 1913-1917.
96. L. Wei, H. Han, J. Shen, *Int. J. Hydrogen Energy* 38 (2013) 11110-11116.
97. Y. Zhang, J. Sun, Y. Hu, Z. Wang, S. Li, *Int. J. Hydrogen Energy* 39 (2014) 8048-8054.
98. M. Ma, Y. Dai, J.L. Zou, L. Wang, K. Pan, H.G. Fu, *ACS Appl. Mater. Interfaces* 6 (2014) 13438-13447.
99. E. Mshoperi, R. Fegel, J. Limson, *Electrochim. Acta* 128 (2014) 311-317.
100. N.A.G. Gomez, I.B. Renteria, D.I.G. Gutierrez, H.A. Mosqueda, E.M. Sanchez, *Mater. Sci. Eng.* B 193 (2015) 130-136.
101. Y. Zhang, J. Sun, Y. Hu, S. Li, Q. Xu, *Int. J. Hydrogen Energy* 37 (2012) 16935-16942.
102. R. Karthikeyan, B. Wang, J. Xuan, J.W.C. Wong, P.K.H. Lee, M.K.H. Leung, *Electrochim. Acta* 157 (2015) 314-323.
103. K.S. Kumar, O.S. Feria, J.T. Ramirez, N.R. Seijas, H.M.P. Varaldo, *Int. J. Hydrogen Energy* 38 (2013) 12600-12609.
104. C. Choi, N. Hu, *Bioresour. Technol*. 133 (2013) 589-598.
105. W. Guo, Y. Pi, H. Song, W. Tang, J. Sun, *Colloids and surfaces A: Physicochem. Eng. Aspects* 415 (2012) 105-111.
106. Z. He, J. Liu, Y. Qiao, C.M. Li, T.T.Y. Tan, *Nano Lett*., 12 (2012) 4738-4741.
107. R.K. Goud, S.V. Mohan, *Int. J. Hydrogen Energy* 36 (2011) 13753-13762.
108. Y. Zhang, J. Sun, B. Hou, Y. Hu, *J. Power Sources* 196 (2011) 7458-7464.
109. K.Y. Cheng, R.C. Ruwisch, G. Ho, *Bioelectrochemistry* 74 (2009) 227-231.
110. M. Sharma, P. Jain, J.L. Varanasi, B. Lal, J. Rodriquez, J.M. Lema, P.M. Sharma, *Bioresour. Technol.* 150 (2013) 172-180.

111. Y. Zhang, J. Sun, Y. Hu, S. Li, Q. Xu, *J. Power Sources* 239 (2013) 169-174.
112. M. Sun, Z.X. Mu, Y.P. Chen, G.P. Sheng, X.W. Liu, Y.Z. Chen, Y. Zhao, H.L. Wang, H.Q. Yu, L. Wei, F. Ma, *Environ. Sci. Technol*. 43 (2009) 3372-3377.
113. Y. Liu, H. Liu, C. Wang, S.X. Hou, N. Yang, *Environ. Sci. Technol*. 47 (2013) 13889-13895.
114. G. Gnana kumar, Z. Awan, K.S. Nahm, J.S. Xavier, *Biosens. Bioelectron*. 53 (2014) 528-534.
115. X. Xia, J.C. Tokash, F. Zhang, P. Liang, X. Huang, B.E. Logan, *Environ. Sci. Technol*. 47 (2013) 2085-2091.
116. Y. Su, Y. Zhu, X. Yang, J. Shen, J. Lu, X. Zhang, J. Chen, C. Li, *Ind. Eng. Chem. Res* 52 (2013) 6076-6082.
117. X. Xia, F. Zhang, X. Zhang, P. Liang, X. Huang, B.E. Logan, *ACS Appl. Mater. Interfaces* 5 (2013) 7862-7866.
118. T. Yin, Z. Lin, L. Su, C. Yuan, D. Fu, *ACS Appl. Mater. Interfaces* 7 (2015) 400-408.
119. X.W. Liu, Y.X. Huang, X.F. Sun, G.P. Sheng, F. Zhao, S.G. Wang, H.Q. Yu, *ACS Appl. Mater. Interfaces* 6 (2014) 8158-8164.
120. G. Gnana kumar, C.J. Kirubaharan, S. Udhayakumar, C. Karthikeyan, K.S. Nahm, *Ind. Eng. Chem. Res* 53 (2014) 16883-16893.
121. S. Liu, H. Song, S. Wei, F. Yang, X. Li, *Bioresour. Technol*. 166 (2014) 575-583.
122. S. Oh, B. Min, B.E. Logan, *Environ. Sci. Technol*. 38 (2004) 4900-4904.
123. X. Xie, L. Hu, M. Pasta, G.F. Wells, D. Kong, C.S. Criddle, Y, Cui, *Nano Lett*. 11 (2011) 291-296.
124. D. Huan, W.Y. Cheng, Z. Fan, H.Z. Chuan, C. Zheng, X.H. Juan, Z. Feng, *Pedosphere* 24 (2014) 330-338.
125. K.P. Katuri, A.M. Enright, V.O. Flaherty, D. Leech, *Bioelectrochemistry* 87 (2012) 164-171.